The Molecular Mechanisms of Testosterone Depletion during Skeletal Myogenesis

Connor Geraghty

Honors Thesis

College of Arts and Sciences, Department of Chemistry

April 13, 2015

A. Background

I. Prostate Cancer

Functional movement is something many healthy people take for granted. Being able to move effectively and confidently is a commodity many men in the US are not able to enjoy. With prostate cancer (PCa), men may experience significant muscle weakness and negative impacts on quality of life due to the treatments used to manage advanced disease [1]. The underlying mechanisms for the growth of the cancerous prostate tumor are based upon testosterone (T) signaling and the conversion of T to dihydrotestosterone (DHT)[2]. Thus, the removal or blocking of T signaling is crucial in slowing the growth of these cancerous lesions[2]. However, T signaling is important to maintaining a number of physiologic processes, including skeletal muscle function[3]. In 2015 the American Cancer Society predicts that 220,800 new cases of PCa will develop, and 27,540 men will die from PCa in the United States alone. One in seven men will be diagnosed with prostate cancer during his lifetime[4], and the risk of developing PCa increases over one thousand fold from age 40-70[5]. For men that progress to metastatic disease the primary treatment is androgen deprivation therapy (ADT), resulting in this population suffering from systemic muscle weakness. Therefore, we aim to investigate the underlying mechanisms associated with testosterone depletion on skeletal muscle.

II. Androgen Signaling

Androgens play a vital role in a large signaling cascade that is initiated within the hypothalamus. The hypothalamus is signaled by androgens, in a feedback manner, to produce luteinizing hormone-releasing hormone (LHRH). LHRH exits the hypothalamus and binds to the LHRH-Receptor (LHRH-R) in the pituitary gland. This binding starts the production of luteinizing hormone (LH), which then travels to the testis to induce the conversion of cholesterol into testosterone. Testosterone is now free to travel to its target tissues, but once it has been brought inside a cell of the target tissue, it must be converted to its active form:

dihydrotestosterone (DHT). From here, DHT can bind to the androgen receptor (AR), and the AR migrates into the nucleus in order to control genes involved in growth, differentiation, and a multitude of other functions[2].

Figure 1: Systemic androgen signaling.

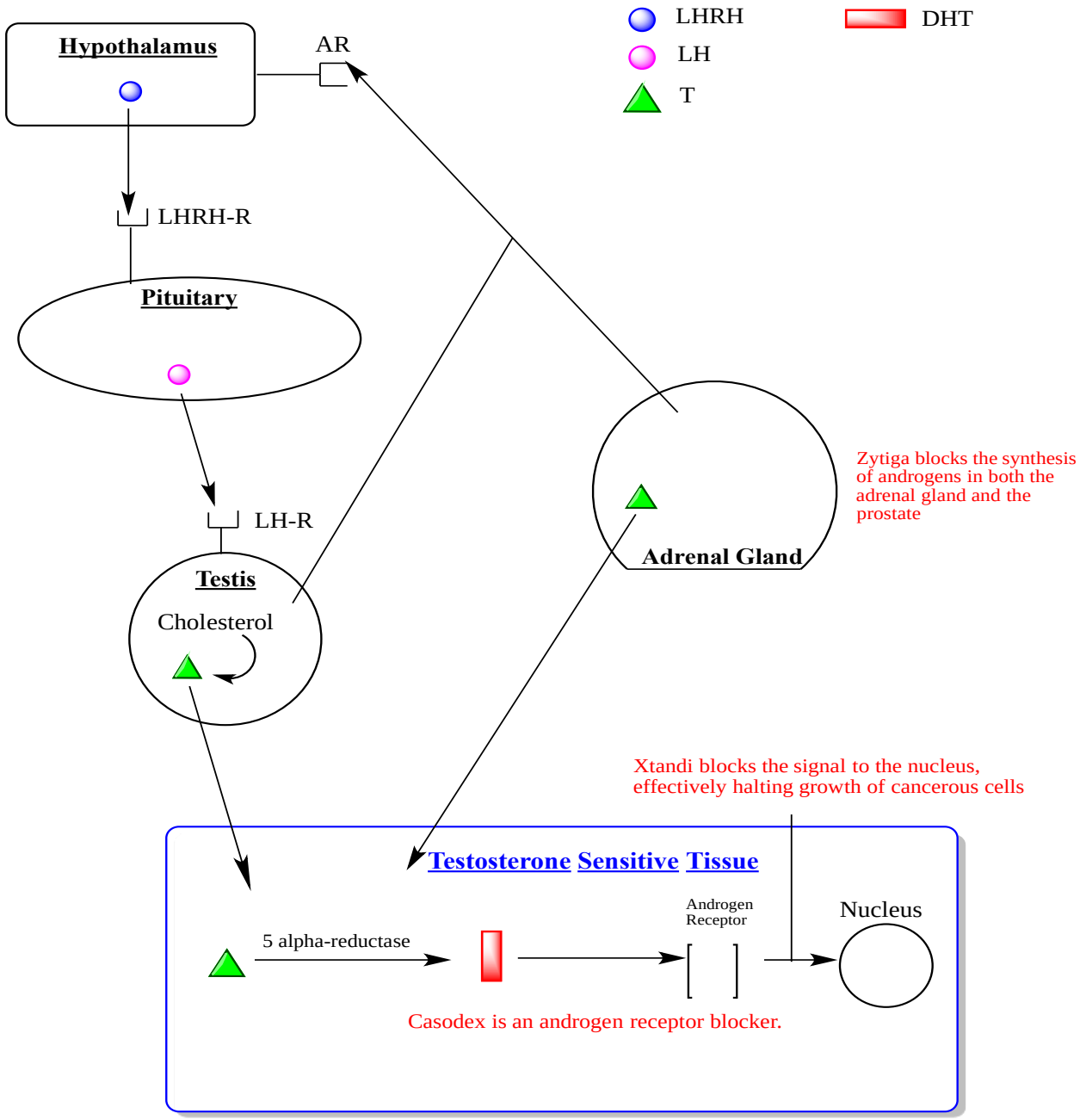

ADT drugs act in several ways relative to the androgen signaling process. The first is to inhibit the production of testosterone all together. The second is to block binding of DHT to the AR within the cytoplasm, and the third is to halt the signal from the AR to the nucleus.

III. Muscle Cells

Muscle cells start out as quiescent satellite cells; small mononuclear muscle precursor cells. External stimuli, such as muscle damage, activate these satellite cells - marked by Pax7 expression - to produce another quiescent satellite cell, and a committed progenitor cell [7]. The progenitor cells start to express Myf5 along with Pax7 as they move into the cell cycle. Once the precursor cells enter into the cell cycle MyoD is up-regulated[6]. The determined state of the muscle cell is the myoblast, which continues to proliferate marked by the expression of Pax7, MyoD, and Myf5 [7]. The myoblasts exit the cell cycle, and enter into the differentiation phase through the down-regulation of cyclin D1, Myf5 and Pax7 [6][7]. The differentiation program is marked by the up-regulation of myogenin, along with the continued expression of MyoD. The myoblasts begin to fuse to form multinucleated myotubes. The differentiation transcription factor myogenin, and the proliferation transcription factor Pax7 are mutually exclusive in their expression[6], and are key markers of the individual processes.

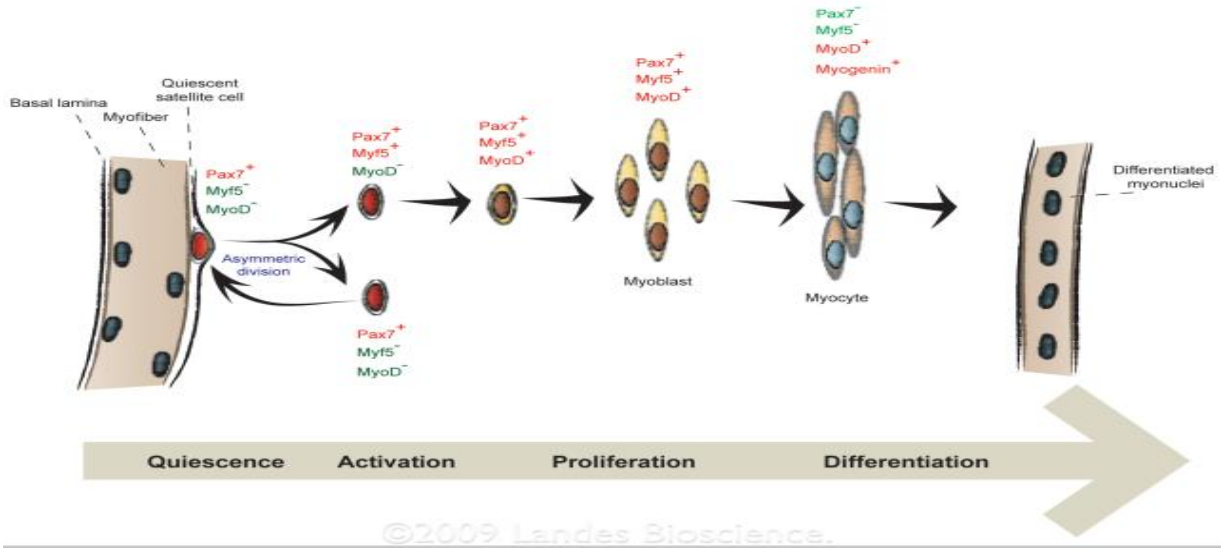

Figure 2: Myoblast activation, proliferation, and differentiation – along with transcriptional markers of the processes [7].

IV. Testosterone and Muscle

Testosterone (T), an androgen, plays a vital role in lean muscle mass growth and strength. A study done on the effects of T supplementation in hypogondal men ranging in age from 21-47, shows that T supplementation not only raises the amount of lean muscle mass by 9%, but also increases strength by 22%[8].

There is evidence that testosterone plays a key role in mediating myoblast proliferation, differentiation, and protein synthesis [9] [10]. Introduction of dihydrotestosterone (DHT) – the active form of testosterone - to a culture of C2C12 cells significantly induced proliferation of the myoblasts[11]. In another study, T introduction during proliferation causes little growth changes[9], but when those same cells were transfected with flag-tagged AR, the myoblast proliferation was inhibited up to 50%. Lee et al. posited the explanation that the AR signaling pathway suppressed the myoblast proliferation. The differentiation of those same cells was

analyzed, and it was concluded that the AR pathway along with T treatment led to up-regulation of myogenin, and accelerated myoblast differentiation [9].

V. Inhibited Testosterone Signaling and its Physiological Effects

ADT drugs are effective at lowering the concentrations of androgens, or inhibiting the AR signaling cascade[12]. The lowering of effective testosterone within a system leads to physiological effects. These physiological effects lead to functional declines, such as weakness, loss of muscle mass, and fat gain[4]. Alibhai et al quantified the functional declines of patients on ADT[1]. The authors measured three functional movements: a six-minute walk test, a grip strength test, and a timed-up-and-go test, in order to simulate effective movement, upper extremity strength, and core strength respectively. The timed-up-and-go test was the amount of time it took a person to stand up from a chair and begin to walk, the grip strength measured the force imparted by the man's grip, and the six-minute walk test measured the distance traveled in six minutes. Patients on ADT performed significantly worse on both the grip strength and timed-up-and-go tests as compared to prostate cancer controls, and healthy controls, and exhibited a trend of worsened performance in the six-minute walk test.

In a review by Storer, et al the authors looked at various studies to assess the strength and functional performance of prostate cancer patients on ADT[13]. Grip strength in ADT patients was 5% lower than healthy controls, ADT patients were an average of 0.24 seconds slower in a walking test and ADT patients were significantly slower in completing 5 chair stands. The decrease in strength in patients undergoing ADT leads to a lower quality of life. Combined, these studies demonstrate a clear systemic impact of ADT on muscle function.

VI. Pre-Clinical Systems to Study the Effect of Low Testosterone on Skeletal Muscle

We aim to investigate the impact of low testosterone status in comparison with clinically relevant pharmacologic agents on myoblast proliferation and differentiation, and their associated mechanisms. Understanding the underlying mechanisms will provide insight into future strategies for limiting these adverse effects, such as with exercise or targeted therapies. There are a variety of well-established pre-clinical systems available to conduct preliminary studies. The C2C12 line is a model of mouse skeletal myoblasts that were originally harvested from the thigh muscle of a two-month-old female mouse. There is a well-established protocol for *in vitro* proliferation and differentiation using this model that makes the C2C12 cell culture system an invaluable tool in order to study the molecular effects of low testosterone status[14]. Figure 2 shows the three main ways that molecular mechanisms of action are studied in animals. Cell lines were the best option for this analysis, because they remain relatively constant over short periods of time, and they are easy to culture, collect, and analyze. The reproducibility is a very desirable trait of the C2C12 cell line, along with the wealth of literature characterizing this cell line.

Types of Cell Cultures			
Type	**Description**	**Primary Uses**	**Disadvantages**
Primary Cell Cultures	*Cells that have been directly harvested and maintained temporarily in a cell culture system*	*Studying specific organs at the cellular level in cells that have not undergone transformation*	*Isolates cells from their natural "habitat", does not take into account effects from rest of body, difficult to isolate single cell types*
In Vivo	*Living Organism*	*Provides a holistic view of the causes and effects of the subject matter*	*Difficult to isolate the specific functions and mechanisms within individual cell types*
Cell Lines	*Population of immortalized cells*	*Very reproducible system of a single cell type. Investigate individual cell types in isolation, and their cellular processes*	*Immortalized cells can change over time in culture and no longer represent the primary tissue; Can only study the mechanisms of a very specific cell line such as muscle or fatty tissue. Removed from natural "habitat"*

Figure 3: Mediums for studying molecular mechanisms of action.

VII. Proliferation and Differentiation Model of C2C12 Muscle Cells

The proliferation and differentiation model of the C2C12 cell system is well defined, and can be monitored via several mechanisms. Proliferating C2C12 myoblasts are supplemented with 10-20% fetal bovine serum (FBS), and allowed to grow until ~80-90% confluent. Once the desired confluencey is reached, the myoblasts are traditionally switched to a 1-3% horse serum (HS) media. The reduction in nutritional content in the media forces the myoblasts out of the cell cycle, and induces differentiation. During differentiation the myoblasts fuse to one another to form multinucleated myotubes.

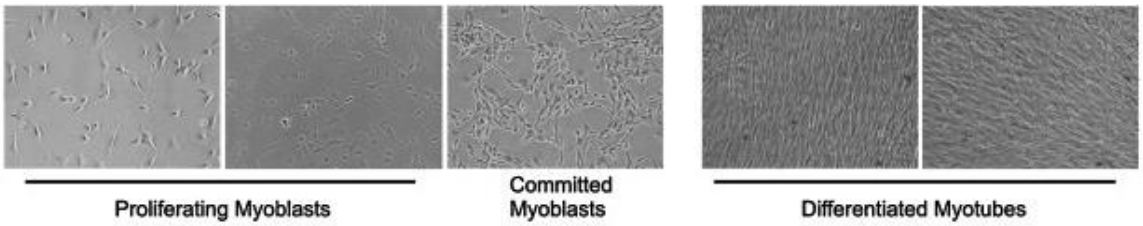

Figure 4: Picture of myogenesis: proliferation of myoblasts through differentiation into myotubes[14].

VIII. Tools to Evaluate Proliferation and Differentiation

Analysis of proliferative progress is most commonly done with an absorbance assay. The cells are treated with certain reagents that interact with a protein, ATP, etc. and the more abundant the target molecule, the greater the theoretical number of cells, and thus a larger absorbance value.

Fully differentiated myotubes can be analyzed through counting of multinucleated myotubes. This gives a relative number of myoblasts that have fused, and helps quantify the extent of differentiation within a culture.

Gene expression patterns during the proliferation and differentiation phases are exclusively unique, and well defined. Cyclin D1 and p21 both mediate cell cycle phase transitions during proliferation, while myogenin and GRIP-1 are key markers of differentiation. The myosin heavy chain isoforms are characteristic of fully differentiated myotubes. By measuring the relative expressions of these genes at various time points, the stages of growth and fusion of myoblasts can be monitored[14].

IX. Proteomics

Proteomic analysis of the cells at various time points furthers the depth of knowledge of cell status. The proteome of the C2C12 system has recently been defined[15]. Proteomics is utilized to identify key proteins that point to the status of the culture as a whole; whether the cells are proliferating and differentiating unhindered, or whether the cell cultures are undergoing some sort of stress from treatment. The inherent depth of proteomic analysis allows for wide spectrum examination of key protein changes or analysis of consistent protein expression during the time course.

B. Hypothesis

We hypothesize that low testosterone status will alter the myoblast proliferation and differentiation processes necessary for sustained skeletal muscle function.

C. Experimental Design and Aims

I. Specific Aims

Specific aim 1: We hypothesize that there will be key pathway changes within the C2C12 myoblast proliferation and differentiation program. (20% fetal bovine serum (FBS) during proliferation, 2% FBS during differentiation.)

Sub-Aim 1: To determine if substituting 2% FBS for 2% horse serum (HS) during differentiation is a sufficient mean of inducing differentiation.

Sub-Aim 2: To examine the proteomic profile, and identify the key pathway changes of the differentiation process.

Specific aim 2: We hypothesize that low testosterone status will effect the myoblasts on a molecular level.

Sub-Aim 1: To determine the pathway changes associated with low testosterone status on the C2C12 culture.

Sub-Aim 2: To establish the molecular implications of low testosterone status on the C2C12 culture.

II. Research Strategies and Methods

Experiment 1: The pilot study of the differences between 2% HS and 2% FBS to induce differentiation was run under general cell culture conditions with 2% HS (Atlanta Biologicals, S12195, Lawrenceville, GA) for one culture of cells to induce differentiation, and 2% FBS to induce differentiation in another. Cell aliquots were collected from time points: -24h through 96h, and analyzed using qRT-PCR along with bright field images at 4x, 10x, 20x, and 40x magnification.

The determination of the key pathways involved in the proliferation and differentiation of muscle cells was accomplished via analysis of the proteomic profile, qRT-PCR array of total RNA, and image collection. Cell pellets from -48h through 96h were collected. The proteome of the -24, 0h, 48h and 96h time points was analyzed, and the -24h, 0h, and 96h time points were analyzed with a qRT-PCR Array.

Parameters Measured							
Time Period	**-48h**	**-24h**	**0h**	**24h**	**48h**	**72h**	**96h**
Proliferation Assay	X	X	X	X	X	X	X
Gene Array		X	X				X
Proteome		X	X		X		X
Images	X	X	X	X	X	X	X

Figure 5: Parameters measured and the time period - for the standard proliferation and differentiation protocol.

Experiment 2: The effects of testosterone depletion in culture were examined proteomically and transcriptionally. These results were augmented with cell viability testing via the cell proliferation assay. Four treatment groups were tested: control group (C), removal of testosterone during proliferation (P), removal during differentiation (D), and removal throughout the entire time course (PD). Charcoal stripped FBS was used in place of regular FBS during the periods of testosterone removal. Cells proliferated on 10 cm tissue plates from -48h to 0h. Differentiation was induced at the 0h time point by switching the cultures to 2% media. The cells were allowed to differentiate through 96h, with media being refreshed every 24 hours. Cell pellets were collected every 24 hours for the entirety of the time course.

Parameters Measured							
Time Period	**-48h**	**-24h**	**0h**	**24h**	**48h**	**72h**	**96h**
Proliferation Assay	X	X	X	X	X	X	X
Gene Array		X	X				X
Proteome		X	X				X
Images	X	X	X	X	X	X	X

Figure 6: Parameters measured and the time period - for the testosterone depletion study of proliferation and differentiation.

Cell Culture Conditions and Reagents: C2C12 mouse skeletal myoblasts (American Type Culture Collection, CRL-1772, Manassas, VA) were plated at $1.5x10^5$ cells per plate at -72h, and maintained in 10 mL of a 20% FBS (Omega Scientific, FB-12, Tarzana, CA) in DMEM (American Type Culture Collection, 30-2002, Manassas, VA) containing 0.01% 100x antibiotic/antimycotic, (Gibco, 15240, Grand Island, NY) and termed growth media (GM). The cultures were kept in a controlled environment at 37^0C, with 5% CO_2 supplementation. The cells proliferated until 90-100% confluent, and were then switched to a differentiation media (DM) of 2% FBS in DMEM from the 0h time point through the terminal 96h time point. Media was refreshed every 24 hours during the entire time course. Images were taken on a bright-field microscope at 4x, 10x, 20x, and 40x magnification for each time point and condition. Cell pellets were subsequently collected, snap frozen in liquid nitrogen, and stored in a -80^0C freezer for downstream analysis.

Proliferation Assay: Cell viability was quantitatively determined using the In Vitro Toxicology Assay Kit, Sulforhodamine B Based (Sigma, TOX6-1KT, St. Louis, MO). 96-well plates were plated with 1750 cells per well - 2 columns (excluding the edges) per condition for the testosterone depletion study - for a total of 8 columns. The cytotoxicity of the treatments was tested per Sigma's manufacturer instructions.

RNA Extraction: Extraction of total RNA was accomplished using the RNeasy Mini Kit (Qiagen, 74106, Maryland), and a QIAshredder (Qiagen, 79054, Maryland) to lyse the cell pellets. All manufacturers' instructions were followed.

Single Gene qRT-PCR: Single gene PCR was run for all time points for the HS vs. FBS study, on the genes listed in Figure 7. cDNA was synthesized via the High Capacity cDNA Reverse Transcription Kit (Applied Biosystems, 4368814, Foster City, CA) according to the

manufacturer's instructions. Subsequent PCR was run utilizing SYBR Green PCR Master Mix (Applied Biosystems, 4309155, Foster City, CA) on MicroAmp Fast Optical 96-wll Reaction Plates (Applied Biosystems, 4346906, China). qRT-PCR was carried out at the Nucleic Acid Shared Resource at The Ohio State University.

Gene Name	Gene Bank Accession #	Sense Primer (5'-3')	Antisense Primer (5'-3')	Gene Function
Cyclophilin	NM0089071	CCCACCGTGTTCTTCGACAT	TTCTCTCCAGTGCTCAGAGC	Accelerates folding of proteins
Myogenin	NM0311891	AGCTGTATGAGACATCCCCC	TTCTTGAGCCTGCGCTTCTC	Myogenin is required to fuse precursor cells to muscle fibers during differentiation
Cyclin D1	NM0076311	CGTGGCCTCTAAGATGAAGG	TGTTCTCATCCGCCTCTGGC	Regulates cell cycle - required for the G1/S transition
p21	U24173	CGGTGGAACTTTGACTTCGT	CAGGGCAGAGGAAGTACTGG	Cyclin dependent kinase inhibitor - mediates G1 and S phases
AR	NM013476	TACCAGCTCACCAAGCTCCT	GATGGGCTTGACTTTCCCAG	Androgen receptor – Critical in many development cunctions
GRIP-1	NM008678	ACAGAACCAGCCAAACCAAC	TGGTTGAGGATTTCCCTCTG	Steroid receptor - Interacts with MEF-2C mediated transcription and formation myotubes - believed to play crucial role in muscle cell differentiation
MyHC-IIb	BC052786	GAGCAGCTGGCGCTGAAGGG	GATTTCTCCTGTCACCTCTC	Predominant Motor protein in skeletal muscle
MyHC IIx/d	XM354615	TCAATGAGCTGACTGCGCAG	CAAGCTGCCTCTTCAGCTCC	Terminally differentiated muscle cell markers (ALL MyHC)
MyHC-I	NM080728	AAGATCGTGTCCCGAGAGGG	TTGTACAGCACAGCCGGCTC	Marker for fully differentiated myotubes

Figure 7: Genes measured with single gene PCR and their function [14].

qRT-PCR Array: The Mouse Skeletal Muscle: Myogenesis and Myopathy RT^2 PCR Array (QIagen, 330231, Maryland) was run for the -24h, 0h, and 96h time points of the testosterone depletion study. cDNA was synthesized per manufacturer's instructions using the RT^2 First Strand Kit (Qiagen, 330401, Maryland). The 384-well plates were prepared according to the manufacturer's directions using RT^2 SYBR Green ROX qPCR Mastermix, (Qiagen, 330521, Maryland) and 400 ng of total RNA from each sample. Samples were run at the OSU Nucleic Acid Shared Resource.

Proteomic Profiling:

Tissue Lysis and Protein Digestion

Cell pellets were digested. Briefly, 100,000 cells were homogenized in a lysis buffer consisting of 9:1 (v/v) ratio of ammonium bicarbonate (50mM) and acetonitrile containing 0.1% (w/v) ProteaseMAX surfactant (Promega, Madison, WI, USA) with the aid of rigorous vortexing. This protein homogenate disulfide bonds were reduced with DTT (5mM) at 56°C, 750RPM for 20 minutes. Reduced disulfide bonds were alkylated with iodoacetamide (10mM) at 25°C in the dark for 30 minutes. Tryptic peptides were produced through digestion with sequence grade trypsin (Promega, Madison, WI, USA) at a ratio of 1:40 (w/w) at 37°C for 9 h under constant agitation (1,000 RPM). ProteaseMAX surfactant was denatured by the addition of 5% formic acid (v/v) then heated at 45°C under constant agitation (800 RPM) for 20 minutes. Peptide mixtures were cleared by centrifugation (21,000xG), dried to dryness using a vacuum centrifugation and resuspended in 0.1% formic acid. Final peptide concentration was determined by 280nm absorbance using a NanoDrop ND-1000 spectrometer (NanoDrop, Wilmington, DE, USA)[16].

Instrument Conditions

Based on 280nm absorbance, 2µg of peptide mixture was separated by reverse phase liquid chromatography (RP-LC). Peptides were desalted at 10uL/min with a trap column, and subsequently separated across an analytical column (0.075 x 150 mm, PepMap C18, 3 µm 100 Å, Thermo Scientific, Waltham, MA). Peptides were introduced into a Velos Pro-ETD dual-pressure linear ion trap mass spectrometer (Thermo Scientific, Waltham, MA) with a EASY-Spray Ion source (Thermo Scientific, Waltham, MA). Two mobile phases were used MPA (0.1% formic acid in HPLC water) and MPB (0.1% formic acid in acetonitrile). Reverse phase analytical separation was completed at 600 nL/min using a 175-minute gradient from 5% to 45% MPB followed by gradient adjustment to 90% MPB over 5 minutes with a 5 minute hold at 90% MPB. Finally the gradient was adjusted to 95% MPB to wash the column and was equilibrated to 5% MPB prior to the next analytical separation. Spray voltage and capillary temperature was set to

1.8 kV and 275°C. A single top-speed data cycle was completed in data-dependent acquisition (DDA) mode consisting of a single full MS scan (AGC target: 30,000 ions; maximum injection time of 150 ms; 1 microscan) followed by 10 MS/MS scans in the linear ion trap (AGC target: 10,000 ions; maximum injection time of 150 ms; 1 microscan). Precursor ions of 1+ charge were rejected. Ion range was confined to 400-1700 m/z with signal abundance above 80,000 TIC were selected for CID fragmentation (35% NCE, q=0.25, 2 m/z isolation width and 10 ms activation time). DDA dynamic exclusion was enabled with a repeat count of one (45s – 1 Da, 45s + 2 Da).

Statistical Methods: In Sigma Plot, expression values for the qRT-PCR array were log transformed (LN) and subsequently tested for normality using the Shapiro-Wilk test. Next the expression values underwent the Brown-Forsythe Equal Variance Test. Pairwise comparisons were made using a 2-way ANOVA with the Holm-Sidak method, with a significance level set to p=0.05[17].

Proteomic data was uploaded to Ingenuity Pathway Analysis (IPA) (Ingenuity Systems), where the data was arranged into predicted pathways based on the fold changes and p-values, as compared to known literature pathways.

D. Results

Investigation into Legitimacy of Fetal Bovine Serum Instead of Horse Serum to induce Differentiation – The traditional method of inducing differentiation in C2C12 myoblasts was to switch from fetal bovine serum (FBS) to adult horse serum (HS) at a low concentration. The reason was the HS had fewer growth factors because it came from an adult, and because HS was provided in a 10-fold lower concentration. The change to a serum with lower amounts of growth factors slowed down the proliferation of the myoblasts, and pushed them towards leaving the cell cycle, and differentiating into multinucleated myotubes. The C2C12 myoblast cell culture system was tested using both 2% HS to induce differentiation, and 2% FBS. The switch to 2% FBS did not drastically alter the phenotypic differentiation program (Fig. 1).

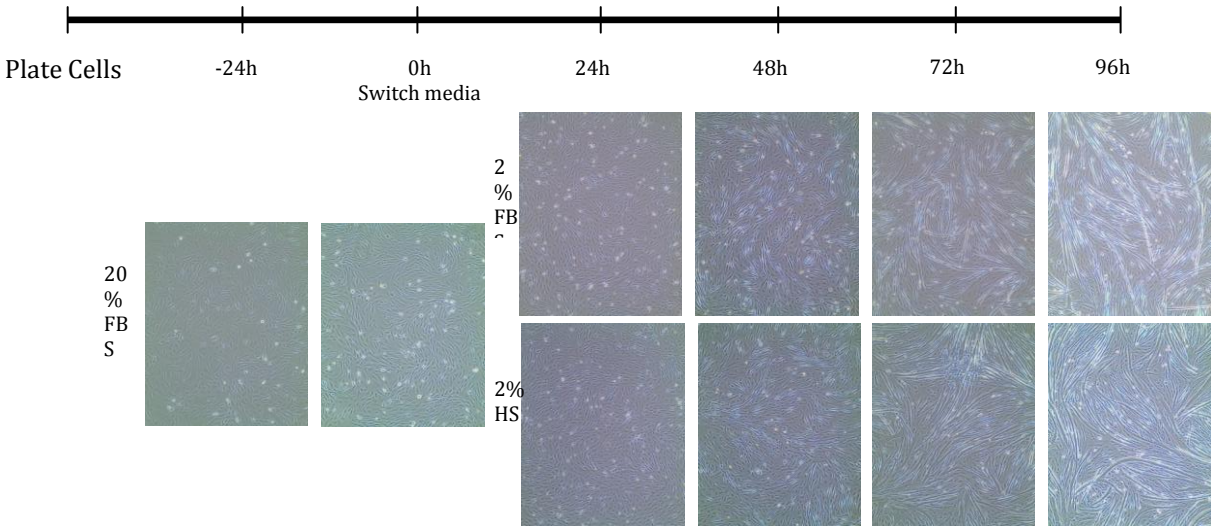

Figure 7: C2C12 culture using 2% FBS vs. 2% HS during differentiation, 40x magnification.

To verify the phenotypic patterns, RNA expression analyses were run on key genes for both the proliferation and differentiation programs. These genes were: Myogenin, Grip-1, Cyclin D1, and MyHC IIx/d. The relative expressions for both the 2% HS and the 2% FBS were very similar for all time points (Fig. 2).

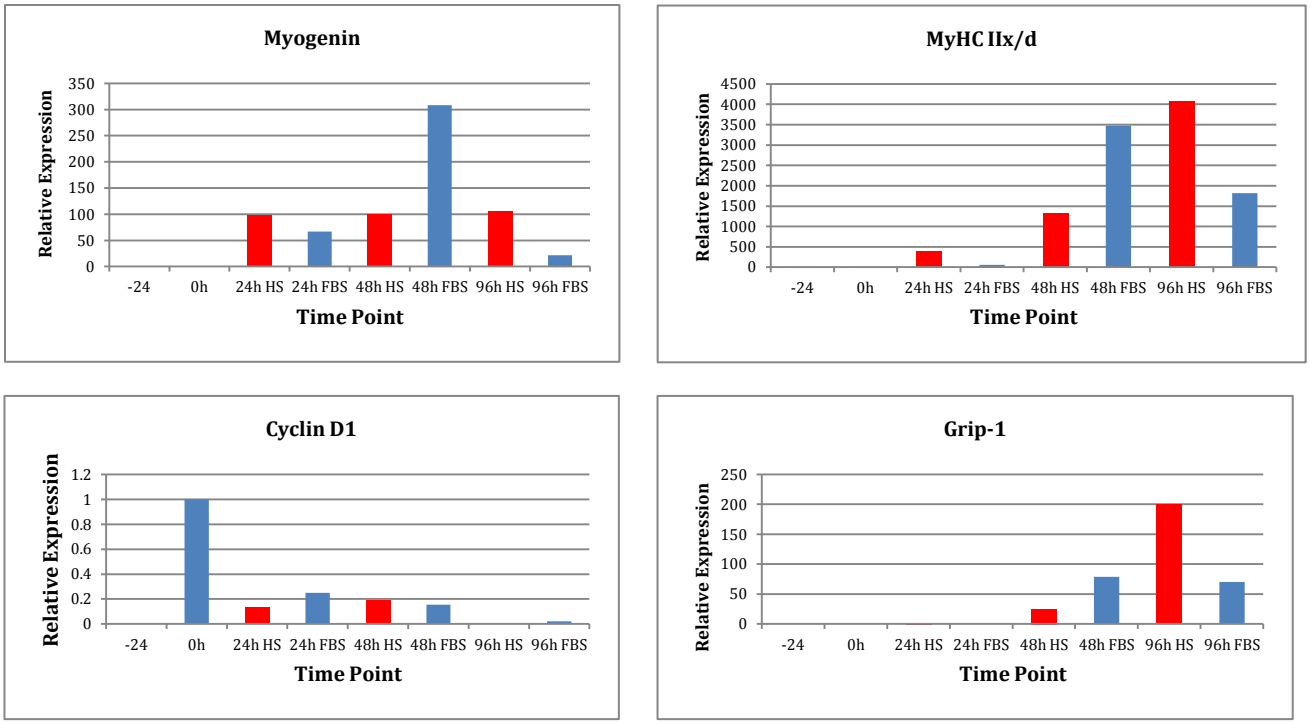

Figure 8: Relative expression ($2^{-(dCT)}$) of 4 key genes throughout the time course relative to the 0h time point. Red represents HS, and blue represents FBS.

The differentiating myoblasts with the 2% FBS followed the trends set by the myoblasts with the 2% HS. Key genes were up- or down-regulated during the same time points. After this initial analysis, it was concluded that the 2% FBS suitably pushed the C2C12 myoblasts into differentiation, and provided an environment conducive to myoblast fusion and myotube formation.

Proteomic Analysis of the C2C12 Differentiation Program – Our proteomic analysis of the C2C12 culture system provided an in-depth look into the pathway effects of differentiation. Three observations were analyzed via the Ingenuity Pathway Analysis software: -24h to 0h, 48h to 0h, and 96h to 0h. These time points are relative to the fully proliferated state of the myoblasts. The -24h to 0h analysis showed the changes during proliferation, the 48h to 0h

showed the early differentiation changes, and the 96h to 0h showed the late differentiation changes.

Starting with the -24h to 0h observation, it was noted that the top canonical pathways for the -24h state relative to the 0h state were epithelial adherens junction signaling, calcium signaling, actin cytoskeleton signaling, and tight junction signaling.

Epithelial Junction Signaling Proteins Present (9/97)			
Symbol	**Gene Name**	**Log ratio**	**p-value**
MYH4	myosin heavy chain 4, skeletal muscle	-5.048	5.44e-04
MYH1	myosin heavy chain 1, skeletal muscle, adult	-4.300	1.64e-02
CTNNB1	catenin beta 1	-1.626	9.35e-02
IQGAP1	IQ motif containing GTPase activating protein 1	-0.425	9.66e-02
MYL1	Myosin light chain 1, skeletal, fast	0	0
MYL3	myosin light chain 3, skeletal, slow	0	0
MYL4	myosin light chain 4, atrial, embryonic	0	0
YES1	YES proto-oncogene 1	0	0
Actn3	actinin alpha 3	0.764	9.04e-2

Calcium Signaling Proteins Present (9/114)			
Symbol	**Gene Name**	**Log Ratio**	**p-value**
MYH1	myosin, heavy chain 1, skeletal muscle, adult	-4.300	1.64e-02
MYH4	myosin, heavy chain 4, skeletal muscle	-5.048	5.44e-04
MYL1	myosin, light chain 1, alkali; skeletal, fast	0.000	0
MYL3	myosin, light chain 3, alkali; ventricular, skeletal, slow	0.000	0
MYL4	myosin, light chain 4, alkali; atrial, embryonic	0.000	0
TNNC2	troponin C type 2 (fast)	0.000	0
TNNI1	troponin I type 1 (skeletal, slow)	0.000	0
TNNT2	troponin T type 2 (cardiac)	0.000	0
TNNT3	troponin T type 3 (skeletal, fast)	0.000	0

Actin Cytoskeleton Signaling Proteins Present (9/128)			
Symbol	**Gene Name**	**Log Ratio**	**p-value**
ACTN3	actinin alpha 3	0.764	9.04e-02
GSN	gelsolin	-0.868	5.00e-02
IQGAP1	IQ motif containing GTPase activating protein 1	-0.425	9.66e-02
MYH1	myosin, heavy chain 1, skeletal muscle, adult	-4.300	1.64e-02
MYH4	myosin, heavy chain 4, skeletal muscle	-5.048	5.44e-04
MYL1	myosin, light chain 1, alkali; skeletal, fast	0.000	0
MYL3	myosin, light chain 3, alkali; ventricular, skeletal, slow	0.000	0
MYL4	myosin, light chain 4, alkali; atrial, embryonic	0.000	0
MYLPF	myosin light chain, phosphorylatable, fast skeletal muscle	0.000	0

Tight Junction Signaling Proteins Present (8/111)			
Symbol	**Entrez Gene Name**	**Log Ratio**	**p-value**
CTNNB1	catenin (cadherin-associated protein), beta 1, 88kDa	-1.626	9.35e-02
MYH1	myosin, heavy chain 1, skeletal muscle, adult	-4.300	1.64e-02
MYH4	myosin, heavy chain 4, skeletal muscle	-5.048	5.44e-04
MYL1	myosin, light chain 1, alkali; skeletal, fast	0.000	0
MYL3	myosin, light chain 3, alkali; ventricular, skeletal, slow	0.000	0
MYL4	myosin, light chain 4, alkali; atrial, embryonic	0.000	0
NAPA	N-ethylmaleimide-sensitive factor attachment protein, alpha	0.000	0
VAPA	VAMP (vesicle-associated membrane protein)-associated protein A, 33kDa	-2.612	3.96e-02

Cellular Effects of Sildenafil Proteins Present (6/62)			
Symbol	**Entrez Gene Name**	**Log Ratio**	**p-value**
MYH1	myosin, heavy chain 1, skeletal muscle, adult	-4.300	1.64E-02
MYH4	myosin, heavy chain 4, skeletal muscle	-5.048	5.44E-04
MYL1	myosin, light chain 1, alkali; skeletal, fast	0.000	0.00E00
MYL3	myosin, light chain 3, alkali; ventricular, skeletal, slow	0.000	0.00E00
MYL4	myosin, light chain 4, alkali; atrial, embryonic	0.000	0.00E00
MYLPF	myosin light chain, phosphorylatable, fast skeletal muscle	0.000	0.00E00

The second observation was the 0h time point relative to the 48h time point. The top pathways were as follows:

Calcium Signaling Proteins Present (19/114)			
Symbol	**Entrez Gene Name**	**Log Ratio**	**p-value**
ACTA1	actin, alpha 1, skeletal muscle	0.366	3.13E-02
ACTA2	actin, alpha 2, smooth muscle, aorta	0.373	3.99E-02
ACTC1	actin, alpha, cardiac muscle 1	0.327	5.61E-02
ATP2A1	ATPase, Ca++ transporting, cardiac muscle, fast twitch 1	2.587	4.85E-04
ATP2A2	ATPase, Ca++ transporting, cardiac muscle, slow twitch 2	2.543	3.29E-04
MYH1	myosin, heavy chain 1, skeletal muscle, adult	3.224	9.77E-04
MYH3	myosin, heavy chain 3, skeletal muscle, embryonic	5.311	1.16E-07
MYH4	myosin, heavy chain 4, skeletal muscle	2.457	2.62E-03
MYH7	myosin, heavy chain 7, cardiac muscle, beta	3.884	3.97E-03
MYH8	myosin, heavy chain 8, skeletal muscle, perinatal	2.720	2.93E-03
MYL1	myosin, light chain 1, alkali; skeletal, fast	6.565	2.07E-07
MYL3	myosin, light chain 3, alkali; ventricular, skeletal, slow	4.117	3.54E-02
MYL4	myosin, light chain 4, alkali; atrial, embryonic	6.076	1.84E-05
TNNC2	troponin C type 2 (fast)	0.000	0.00E00
TNNI1	troponin I type 1 (skeletal, slow)	4.505	8.32E-03
TNNT2	troponin T type 2 (cardiac)	4.950	1.25E-03
TNNT3	troponin T type 3 (skeletal, fast)	4.326	1.76E-02
Tpm1	tropomyosin 1, alpha	1.032	3.67E-04
Tpm2	tropomyosin 2, beta	1.521	7.92E-06

Cellular Effects of Sildenafil Proteins Present (13/62)			
Symbol	**Entrez Gene Name**	**Log Ratio**	**p-value**
ACTA1	actin, alpha 1, skeletal muscle	0.366	3.13E-02
ACTA2	actin, alpha 2, smooth muscle, aorta	0.373	3.99E-02
ACTC1	actin, alpha, cardiac muscle 1	0.327	5.61E-02
GNAS	GNAS complex locus	1.797	6.10E-02
MYH1	myosin, heavy chain 1, skeletal muscle, adult	3.224	9.77E-04
MYH3	myosin, heavy chain 3, skeletal muscle, embryonic	5.311	1.16E-07
MYH4	myosin, heavy chain 4, skeletal muscle	2.457	2.62E-03
MYH7	myosin, heavy chain 7, cardiac muscle, beta	3.884	3.97E-03
MYH8	myosin, heavy chain 8, skeletal muscle, perinatal	2.720	2.93E-03
MYL1	myosin, light chain 1, alkali; skeletal, fast	6.565	2.07E-07
MYL3	myosin, light chain 3, alkali; ventricular, skeletal, slow	4.117	3.54E-02
MYL4	myosin, light chain 4, alkali; atrial, embryonic	6.076	1.84E-05
MYLPF	myosin light chain, phosphorylatable, fast skeletal muscle	4.855	1.18E-02

Epithelial Adherens Junction Signaling Proteins Changes (15/97)			
Symbol	**Entrez Gene Name**	**Log Ratio**	**p-value**
ACTA1	actin, alpha 1, skeletal muscle	0.366	3.13E-02
ACTA2	actin, alpha 2, smooth muscle, aorta	0.373	3.99E-02
ACTC1	actin, alpha, cardiac muscle 1	0.327	5.61E-02
Actn3	actinin alpha 3	1.394	6.37E-03
CTNNA1	catenin (cadherin-associated protein), alpha 1, 102kDa	0.786	8.16E-02
MYH1	myosin, heavy chain 1, skeletal muscle, adult	3.224	9.77E-04
MYH3	myosin, heavy chain 3, skeletal muscle, embryonic	5.311	1.16E-07
MYH4	myosin, heavy chain 4, skeletal muscle	2.457	2.62E-03
MYH7	myosin, heavy chain 7, cardiac muscle, beta	3.884	3.97E-03
MYH8	myosin, heavy chain 8, skeletal muscle, perinatal	2.720	2.93E-03
MYL1	myosin, light chain 1, alkali; skeletal, fast	6.565	2.07E-07
MYL3	myosin, light chain 3, alkali; ventricular, skeletal, slow	4.117	3.54E-02
MYL4	myosin, light chain 4, alkali; atrial, embryonic	6.076	1.84E-05
VCL	vinculin	0.454	9.69E-03
YES1	YES proto-oncogene 1, Src family tyrosine kinase	0.000	0.00E00

ILK Signaling Protein Changes (15/115)			
Symbol	**Entrez Gene Name**	**Log Ratio**	**p-value**
ACTA1	actin, alpha 1, skeletal muscle	0.366	3.13E-02
ACTA2	actin, alpha 2, smooth muscle, aorta	0.373	3.99E-02
ACTC1	actin, alpha, cardiac muscle 1	0.327	5.61E-02
Actn3	actinin alpha 3	1.394	6.37E-03
FLNB	filamin B, beta	-0.609	8.50E-03
FLNC	filamin C, gamma	0.857	1.98E-06
MYH1	myosin, heavy chain 1, skeletal muscle, adult	3.224	9.77E-04
MYH3	myosin, heavy chain 3, skeletal muscle, embryonic	5.311	1.16E-07
MYH4	myosin, heavy chain 4, skeletal muscle	2.457	2.62E-03
MYH7	myosin, heavy chain 7, cardiac muscle, beta	3.884	3.97E-03
MYH8	myosin, heavy chain 8, skeletal muscle, perinatal	2.720	2.93E-03
MYL1	myosin, light chain 1, alkali; skeletal, fast	6.565	2.07E-07
MYL3	myosin, light chain 3, alkali; ventricular, skeletal, slow	4.117	3.54E-02
MYL4	myosin, light chain 4, alkali; atrial, embryonic	6.076	1.84E-05
VIM	vimentin	-0.194	6.38E-02

Actin Cytoskeleton Signaling Protein Changes (15/128)			
Symbol	**Entrez Gene Name**	**Log Ratio**	**p-value**
ACTA1	actin, alpha 1, skeletal muscle	0.366	3.13E-02
ACTA2	actin, alpha 2, smooth muscle, aorta	0.373	3.99E-02
ACTC1	actin, alpha, cardiac muscle 1	0.327	5.61E-02
Actn3	actinin alpha 3	1.394	6.37E-03
MYH1	myosin, heavy chain 1, skeletal muscle, adult	3.224	9.77E-04
MYH3	myosin, heavy chain 3, skeletal muscle, embryonic	5.311	1.16E-07
MYH4	myosin, heavy chain 4, skeletal muscle	2.457	2.62E-03
MYH7	myosin, heavy chain 7, cardiac muscle, beta	3.884	3.97E-03
MYH8	myosin, heavy chain 8, skeletal muscle, perinatal	2.720	2.93E-03
MYL1	myosin, light chain 1, alkali; skeletal, fast	6.565	2.07E-07
MYL3	myosin, light chain 3, alkali; ventricular, skeletal, slow	4.117	3.54E-02
MYL4	myosin, light chain 4, alkali; atrial, embryonic	6.076	1.84E-05
MYLPF	myosin light chain, phosphorylatable, fast skeletal muscle	4.855	1.18E-02
TTN	titin	0.651	6.34E-03
VCL	vinculin	0.454	9.69E-03

The third observation was from the 0h time point to the 96h time point. The top canonical pathways were as follows:

Calcium Signaling Pathway Protein Changes (20/114)			
Symbol	**Entrez Gene Name**	**Log Ratio**	**p-value**
ACTA1	actin, alpha 1, skeletal muscle	0.751	1.50E-08
ACTA2	actin, alpha 2, smooth muscle, aorta	0.810	4.90E-09
ACTC1	actin, alpha, cardiac muscle 1	0.684	1.53E-07
ATP2A1	ATPase, Ca++ transporting, cardiac muscle, fast twitch 1	4.481	2.45E-15
ATP2A2	ATPase, Ca++ transporting, cardiac muscle, slow twitch 2	3.658	1.17E-08
MYH1	myosin, heavy chain 1, skeletal muscle, adult	5.718	1.94E-14
MYH3	myosin, heavy chain 3, skeletal muscle, embryonic	6.875	1.11E-24
MYH4	myosin, heavy chain 4, skeletal muscle	4.760	4.63E-13
MYH7	myosin, heavy chain 7, cardiac muscle, beta	6.559	1.22E-15
MYH8	myosin, heavy chain 8, skeletal muscle, perinatal	5.108	4.77E-18
MYL1	myosin, light chain 1, alkali; skeletal, fast	8.120	1.50E-24
MYL3	myosin, light chain 3, alkali; ventricular, skeletal, slow	5.918	7.27E-07
MYL4	myosin, light chain 4, alkali; atrial, embryonic	7.336	1.59E-15
TNNC2	troponin C type 2 (fast)	4.664	4.25E-03
TNNI1	troponin I type 1 (skeletal, slow)	5.849	1.62E-06
TNNT2	troponin T type 2 (cardiac)	5.920	8.01E-07
TNNT3	troponin T type 3 (skeletal, fast)	5.175	3.12E-04
Tpm1	tropomyosin 1, alpha	1.456	4.06E-08
Tpm2	tropomyosin 2, beta	2.074	8.43E-12
Tpm4	tropomyosin 4	-0.973	7.92E-03

ILK Signaling Protein Changes (18/115)			
Symbol	**Entrez Gene Name**	**Log Ratio**	**p-value**
ACTA1	actin, alpha 1, skeletal muscle	0.751	1.50E-08
ACTA2	actin, alpha 2, smooth muscle, aorta	0.810	4.90E-09
ACTC1	actin, alpha, cardiac muscle 1	0.684	1.53E-07
ACTN2	actinin, alpha 2	0.639	7.35E-02
Actn3	actinin alpha 3	2.172	2.54E-06
FLNA	filamin A, alpha	-0.554	7.31E-02
FLNB	filamin B, beta	-1.217	2.71E-07
FLNC	filamin C, gamma	1.491	1.81E-15
MYH1	myosin, heavy chain 1, skeletal muscle, adult	5.718	1.94E-14
MYH3	myosin, heavy chain 3, skeletal muscle, embryonic	6.875	1.11E-24
MYH4	myosin, heavy chain 4, skeletal muscle	4.760	4.63E-13
MYH7	myosin, heavy chain 7, cardiac muscle, beta	6.559	1.22E-15
MYH8	myosin, heavy chain 8, skeletal muscle, perinatal	5.108	4.77E-18
MYL1	myosin, light chain 1, alkali; skeletal, fast	8.120	1.50E-24
MYL3	myosin, light chain 3, alkali; ventricular, skeletal, slow	5.918	7.27E-07
MYL4	myosin, light chain 4, alkali; atrial, embryonic	7.336	1.59E-15
NACA	nascent polypeptide-associated complex alpha subunit	1.268	1.88E-05
VIM	vimentin	-0.362	1.46E-02

Epithelial Adherens Junction Signaling Protein Changes (16/197)			
Symbol	**Entrez Gene Name**	**Log Ratio**	**p-value**
ACTA1	actin, alpha 1, skeletal muscle	0.751	1.50E-08
ACTA2	actin, alpha 2, smooth muscle, aorta	0.810	4.90E-09
ACTC1	actin, alpha, cardiac muscle 1	0.684	1.53E-07
ACTN2	actinin, alpha 2	0.639	7.35E-02
Actn3	actinin alpha 3	2.172	2.54E-06
MYH1	myosin, heavy chain 1, skeletal muscle, adult	5.718	1.94E-14
MYH3	myosin, heavy chain 3, skeletal muscle, embryonic	6.875	1.11E-24
MYH4	myosin, heavy chain 4, skeletal muscle	4.760	4.63E-13
MYH7	myosin, heavy chain 7, cardiac muscle, beta	6.559	1.22E-15
MYH8	myosin, heavy chain 8, skeletal muscle, perinatal	5.108	4.77E-18
MYL1	myosin, light chain 1, alkali; skeletal, fast	8.120	1.50E-24
MYL3	myosin, light chain 3, alkali; ventricular, skeletal, slow	5.918	7.27E-07
MYL4	myosin, light chain 4, alkali; atrial, embryonic	7.336	1.59E-15
TUBB6	tubulin, beta 6 class V	0.301	9.91E-02
VCL	vinculin	0.563	1.46E-03
YES1	YES proto-oncogene 1, Src family tyrosine kinase	4.107	3.29E-02

Actin Cytoskeleton Signaling Protein Changesz (18/128)			
Symbol	**Entrez Gene Name**	**Log Ratio**	**p-value**
ACTA1	actin, alpha 1, skeletal muscle	0.751	1.50E-08
ACTA2	actin, alpha 2, smooth muscle, aorta	0.810	4.90E-09
ACTC1	actin, alpha, cardiac muscle 1	0.684	1.53E-07
ACTN2	actinin, alpha 2	0.639	7.35E-02
Actn3	actinin alpha 3	2.172	2.54E-06
EZR	ezrin	-0.541	9.07E-02
FLNA	filamin A, alpha	-0.554	7.31E-02
MYH1	myosin, heavy chain 1, skeletal muscle, adult	5.718	1.94E-14
MYH3	myosin, heavy chain 3, skeletal muscle, embryonic	6.875	1.11E-24
MYH4	myosin, heavy chain 4, skeletal muscle	4.760	4.63E-13
MYH7	myosin, heavy chain 7, cardiac muscle, beta	6.559	1.22E-15
MYH8	myosin, heavy chain 8, skeletal muscle, perinatal	5.108	4.77E-18
MYL1	myosin, light chain 1, alkali; skeletal, fast	8.120	1.50E-24
MYL3	myosin, light chain 3, alkali; ventricular, skeletal, slow	5.918	7.27E-07
MYL4	myosin, light chain 4, alkali; atrial, embryonic	7.336	1.59E-15
MYLPF	myosin light chain, phosphorylatable, fast skeletal muscle	7.402	5.21E-11
TTN	titin	1.066	1.66E-03
VCL	vinculin	0.563	1.46E-03

Mitochondrial Dysfunction Proteins Present (17/123)			
Symbol	**Entrez Gene Name**	**Log Ratio**	**p-value**
ACTA1	actin, alpha 1, skeletal muscle	0.751	1.50E-08

ACTA2	actin, alpha 2, smooth muscle, aorta	0.810	4.90E-09
ACTC1	actin, alpha, cardiac muscle 1	0.684	1.53E-07
ACTN2	actinin, alpha 2	0.639	7.35E-02
Actn3	actinin alpha 3	2.172	2.54E-06
EZR	ezrin	-0.541	9.07E-02
FLNA	filamin A, alpha	-0.554	7.31E-02
MYH1	myosin, heavy chain 1, skeletal muscle, adult	5.718	1.94E-14
MYH3	myosin, heavy chain 3, skeletal muscle, embryonic	6.875	1.11E-24
MYH4	myosin, heavy chain 4, skeletal muscle	4.760	4.63E-13
MYH7	myosin, heavy chain 7, cardiac muscle, beta	6.559	1.22E-15
MYH8	myosin, heavy chain 8, skeletal muscle, perinatal	5.108	4.77E-18
MYL1	myosin, light chain 1, alkali; skeletal, fast	8.120	1.50E-24
MYL3	myosin, light chain 3, alkali; ventricular, skeletal, slow	5.918	7.27E-07
MYL4	myosin, light chain 4, alkali; atrial, embryonic	7.336	1.59E-15
MYLPF	myosin light chain, phosphorylatable, fast skeletal muscle	7.402	5.21E-11
TTN	titin	1.066	1.66E-03
VCL	vinculin	0.563	1.46E-03

The predicted top upstream regulators were analyzed along with the top canonical pathways.

The upstream regulators were both identified, and a prediction made on the state of activation.

The top upstream regulators for all time periods as identified by IPA were as follows:

INSR:

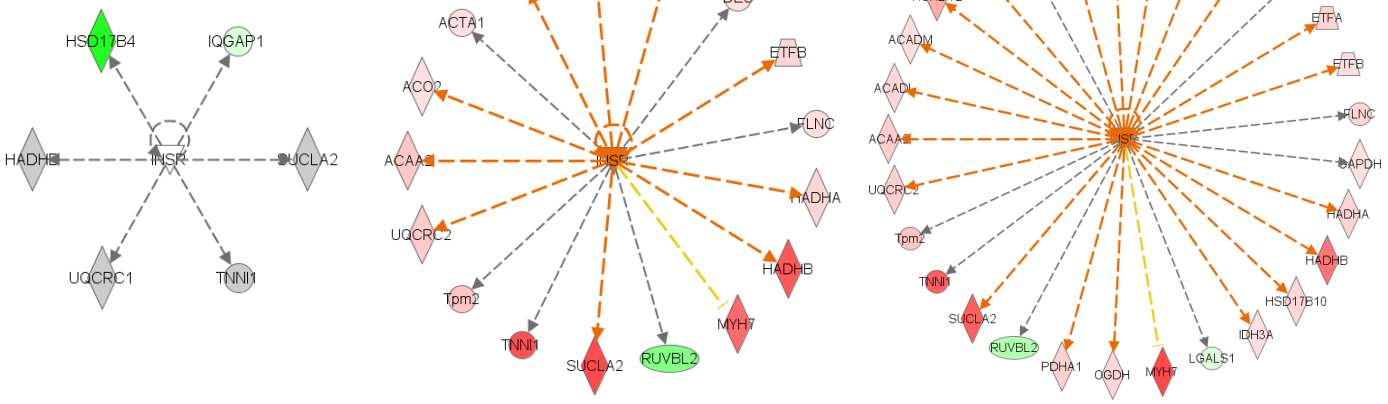

-24h to 0h 48h to 0h 96h to 0h

TP53:

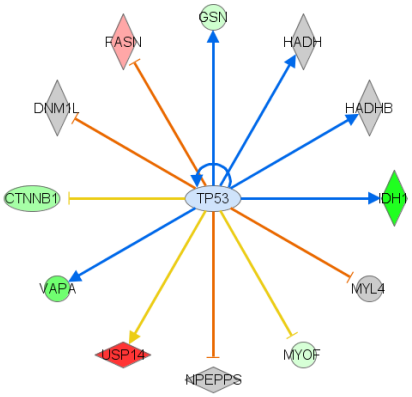

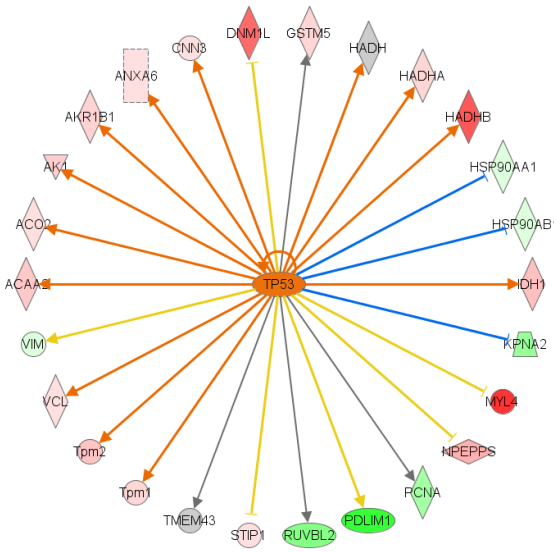

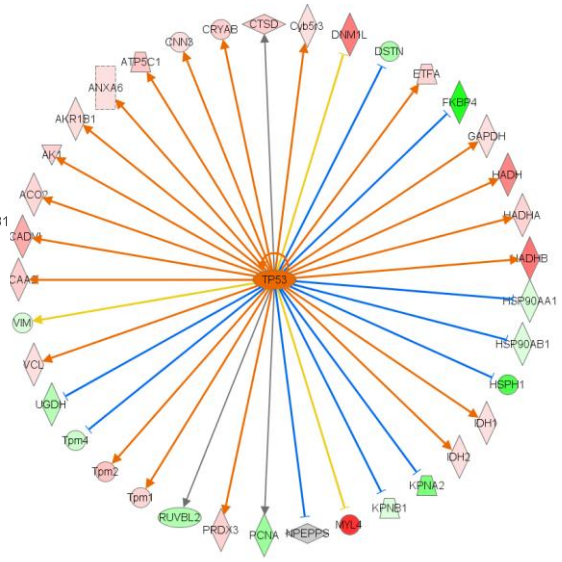

-24h to 0h

48h to 0h

96h to 0h

SRF:

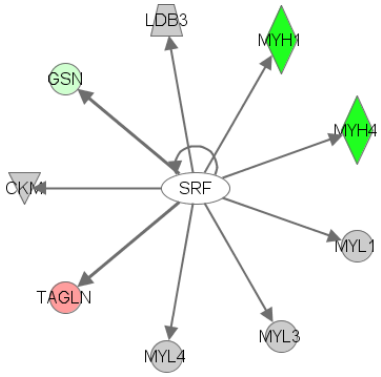

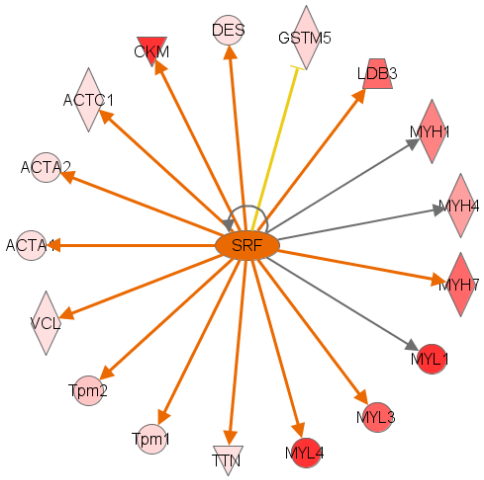

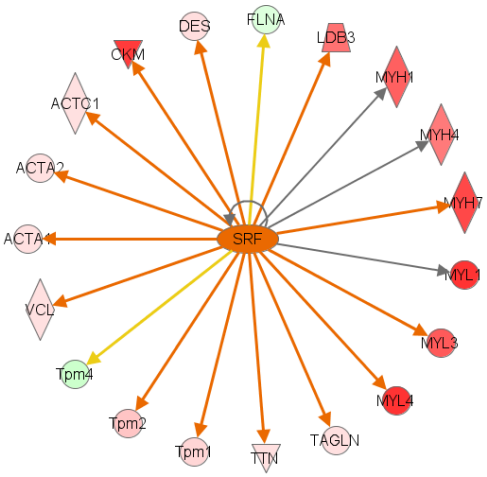

-24h to 0h

48h to 0h

96h to 0h

IGF1R:

NO DATA

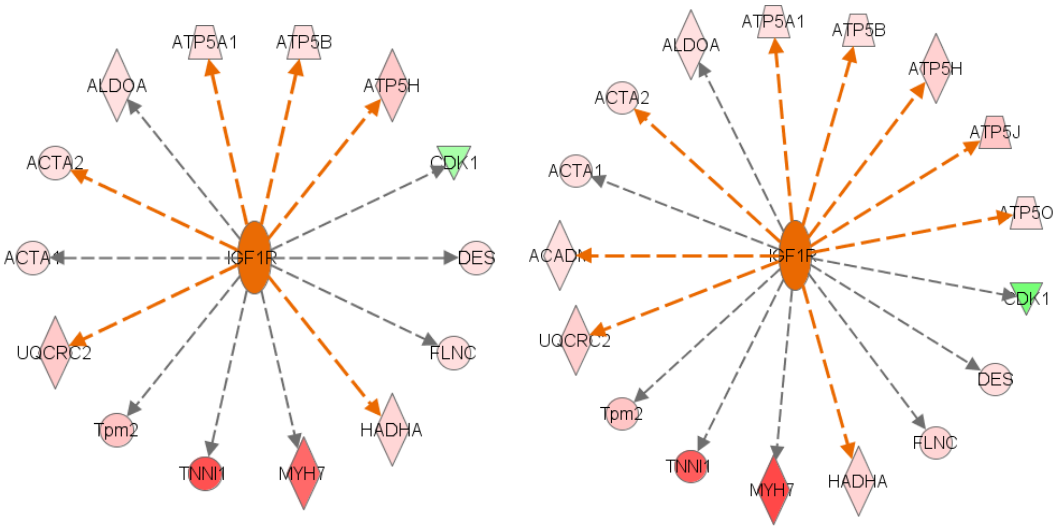

-24h to 0h 48h to 0h 96h to 0h

Figure 9: Top upstream regulators of the differentiation process – pairwise comparison between the time points.

Figure 9 shows the top upstream regulators predicted by IPA. The top regulators of the differentiation process were INSR, TP53, SRF and IGF1R. These molecules regulate the process in various ways, and are critical the differentiation of myoblasts.

Transcriptional analysis of testosterone depletion during the proliferation and differentiation programs - The C2C12 mouse myoblast cells were treated with charcoal stripped FBS (CS-FBS) during the proliferation phase (P), the differentiation phase (D), and throughout the entire time course (PD), as seen in Figure 10.

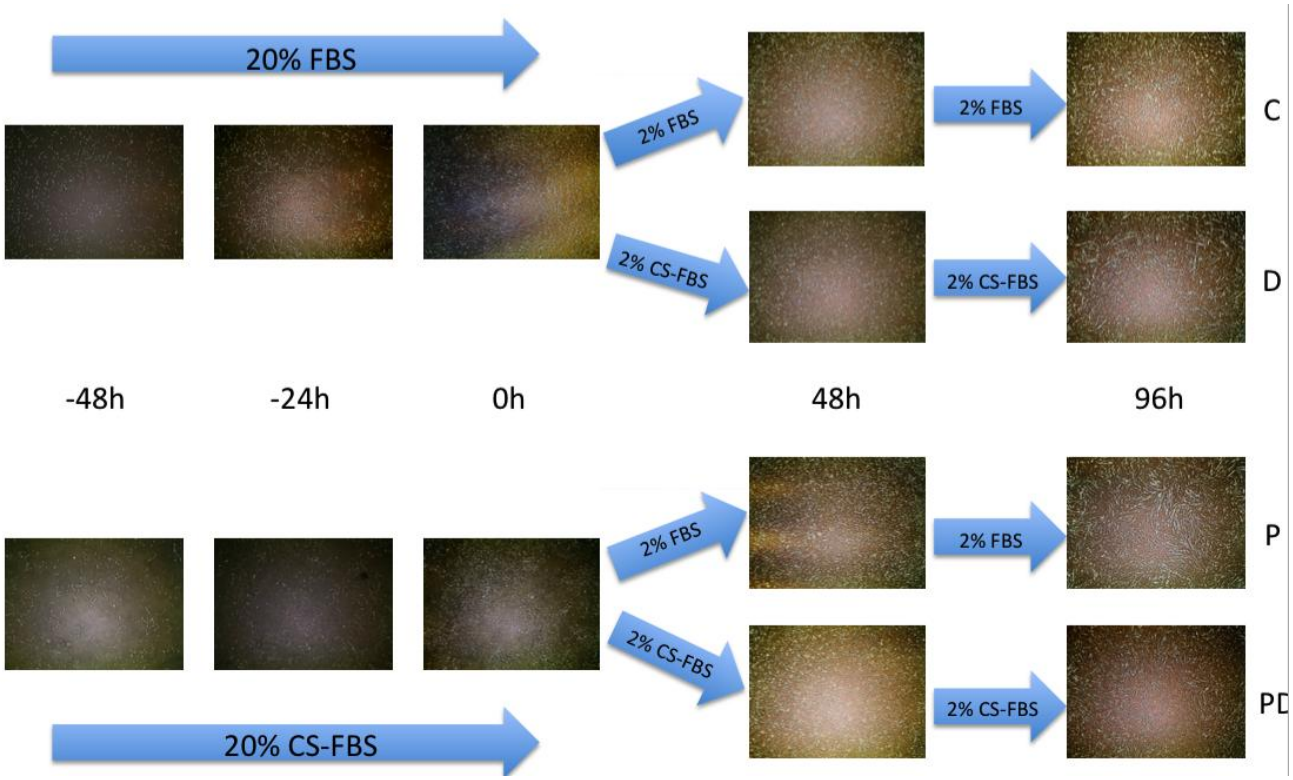

Figure 10: Pictures of the different treatment groups undergoing the differentiation process.

The cells were visually less confluent at 0h after being treated with CS-FBS. When undergoing differentiation, having full media (not charcoal stripped) led to longer myotube formation. A myogenesis PCR array was run to confirm the phenotypic changes. The -24h, 0h, and 96h time points were selected for analysis because they showed the greatest phenotypic changes for the control group. Below are the functional gene groupings along with their relative expressions:

Skeletal Myogenesis:

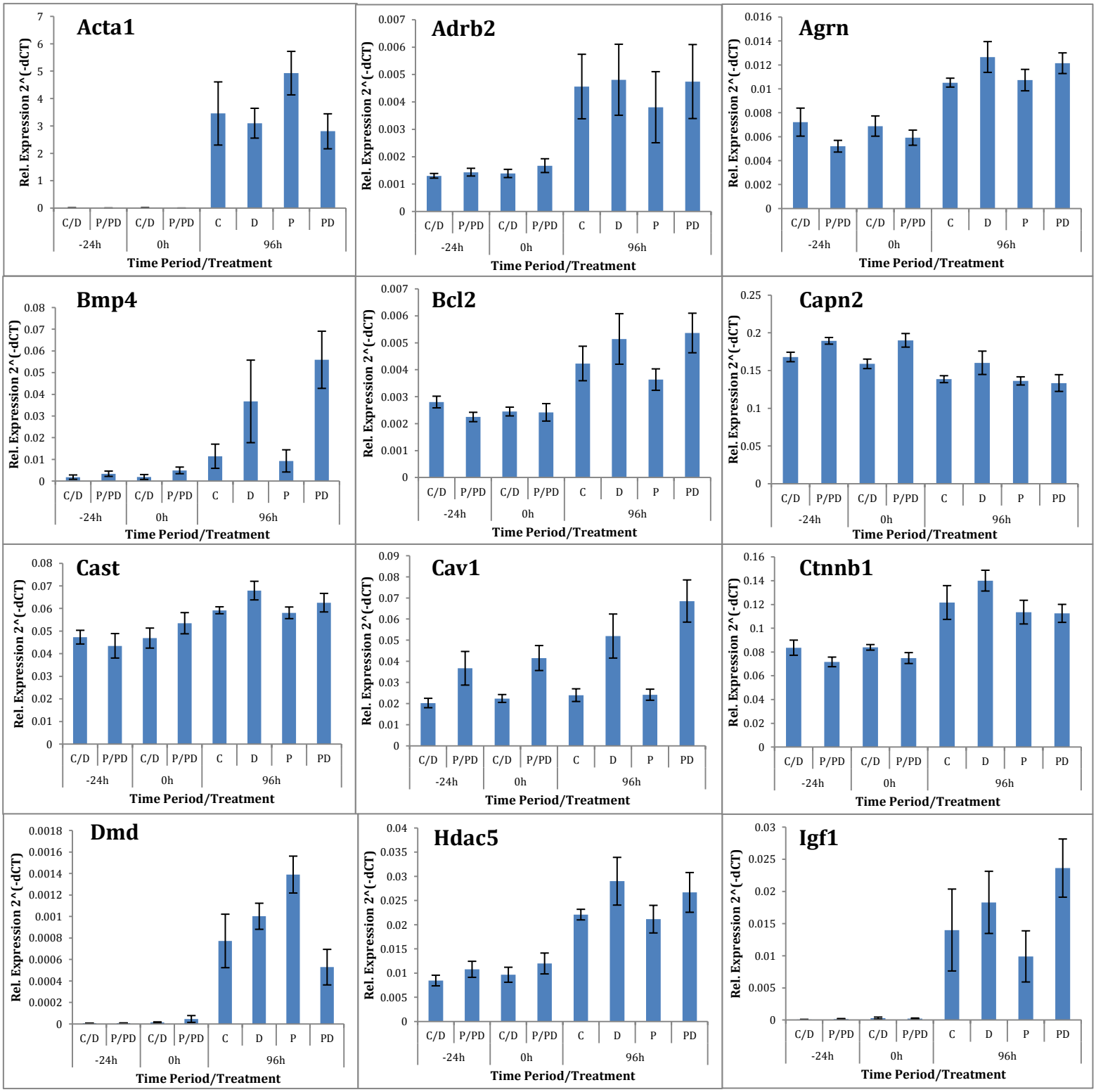

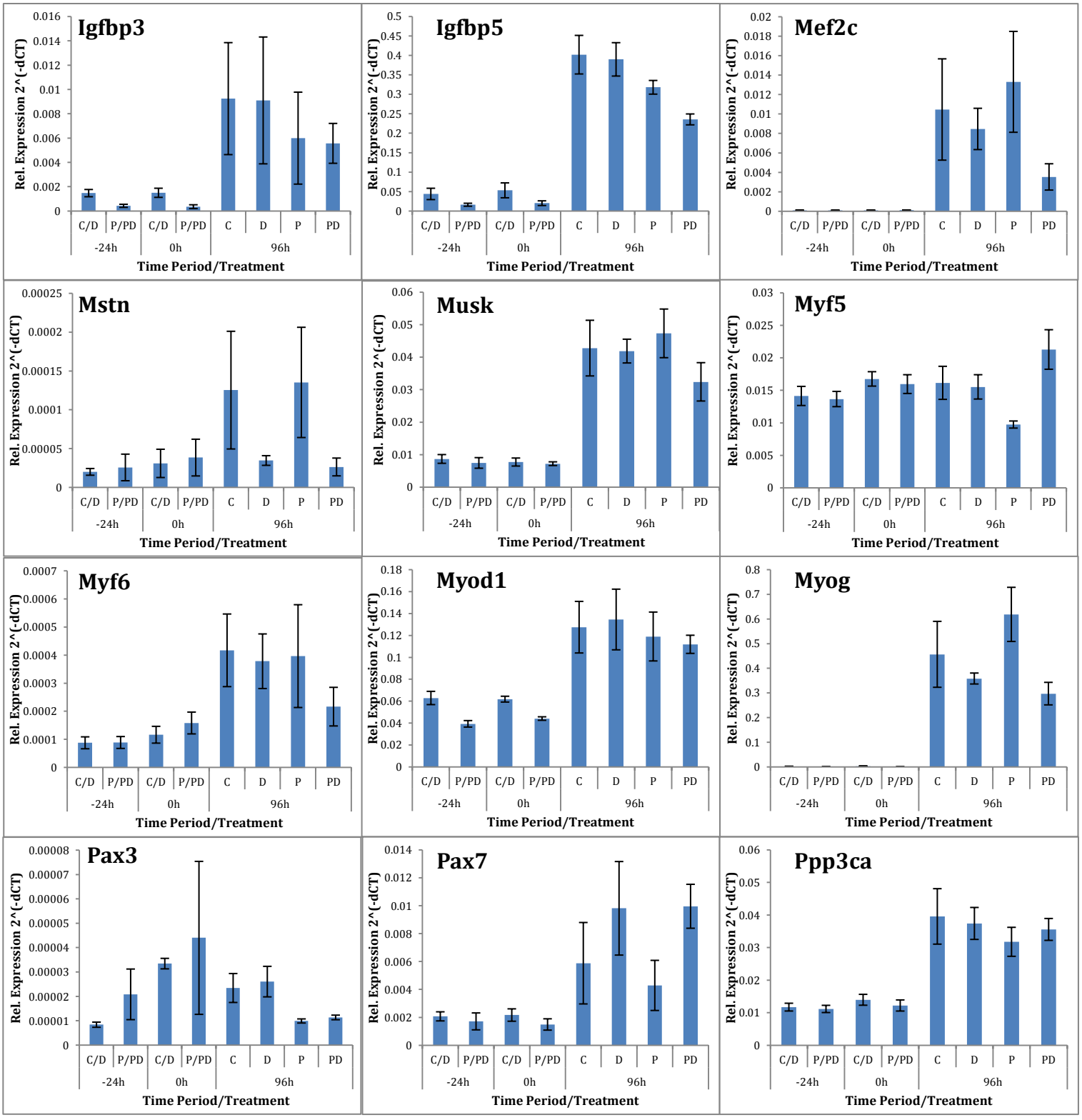
Igfbp3
Igfbp5
Mef2c
Mstn
Musk
Myf5
Myf6
Myod1
Myog
Pax3
Pax7
Ppp3ca
Rel. Expression 2^(-dCT)
C/D
P/PD
C
D
P
PD
-24h
0h
96h
Time Period/Treatment

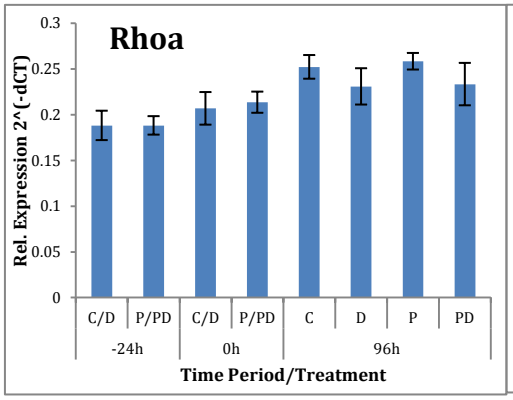

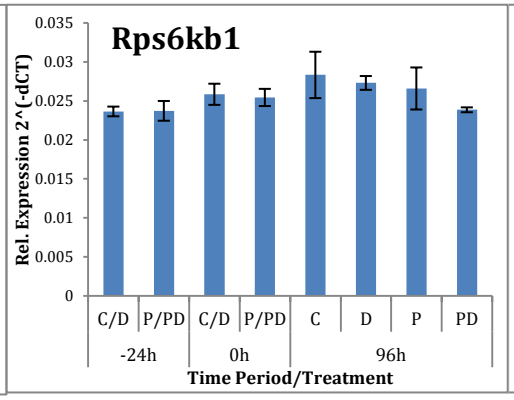

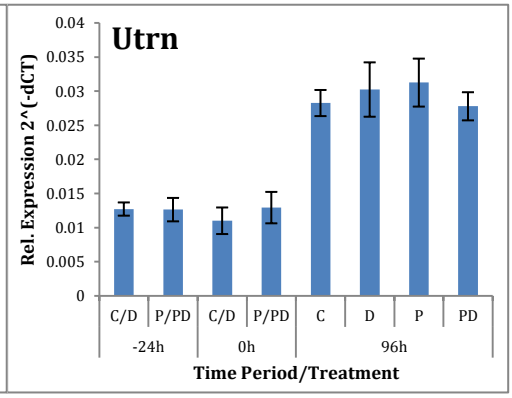

Skeletal Muscle Contractility:

Fast-Twitch Fibers:

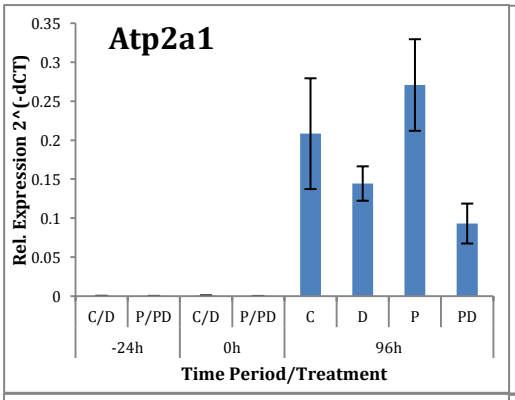

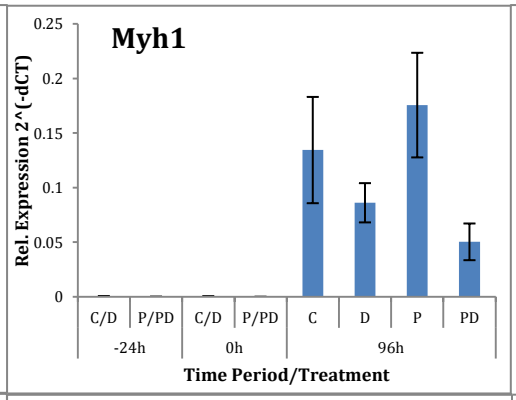

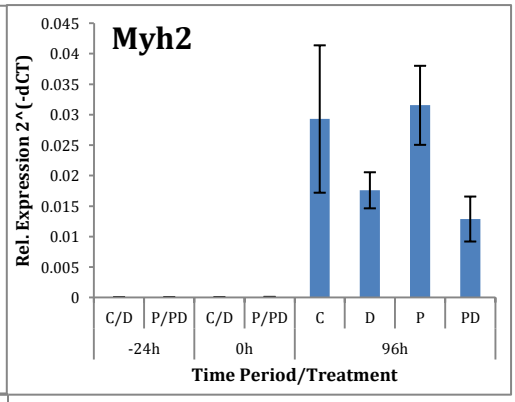

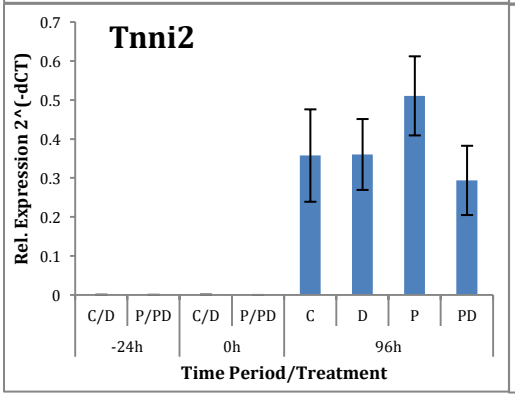

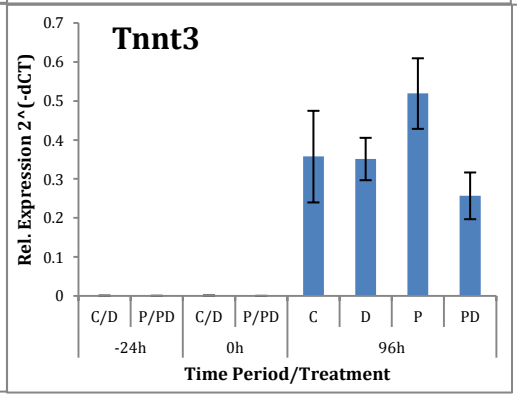

Slow-Twitch Fibers:

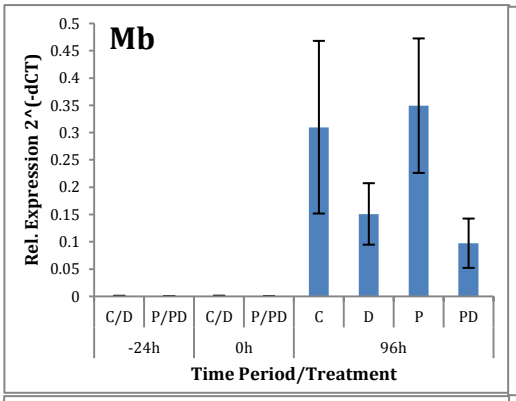

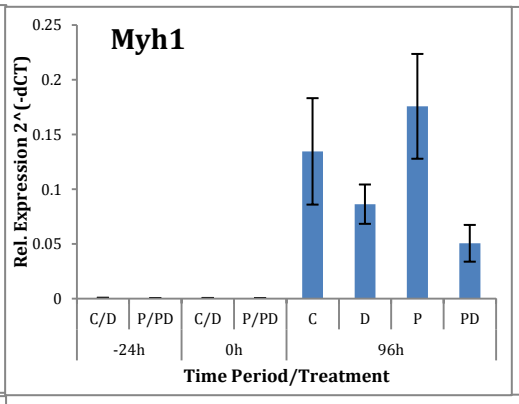

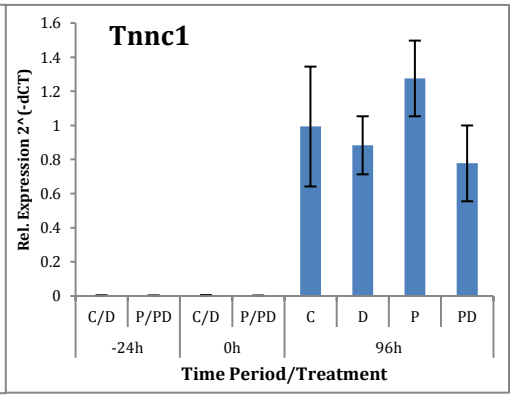

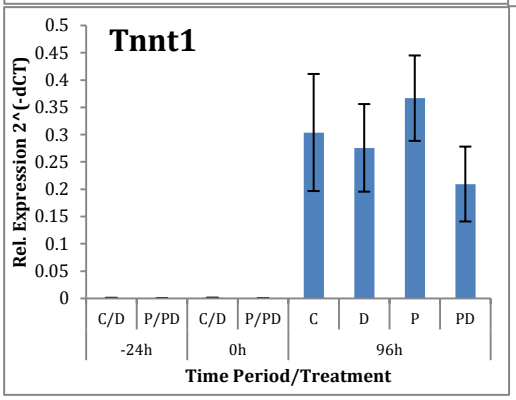

Skeletal Muscle Autocrine Signaling:

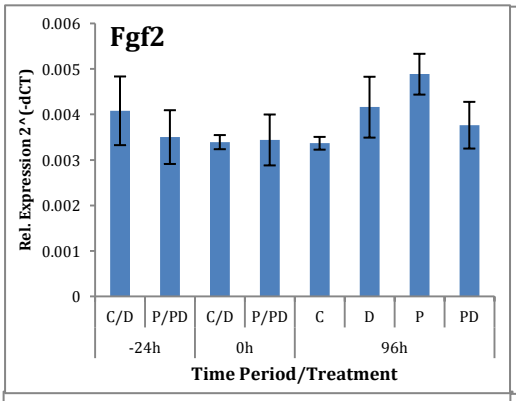

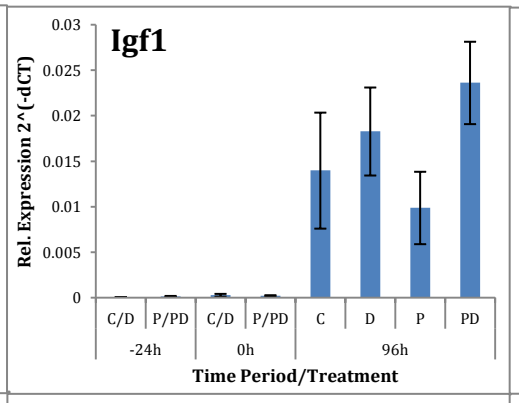

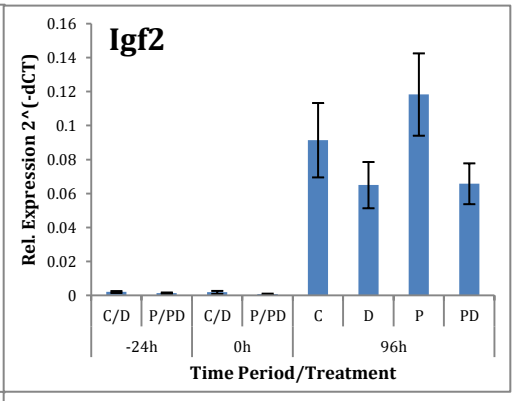

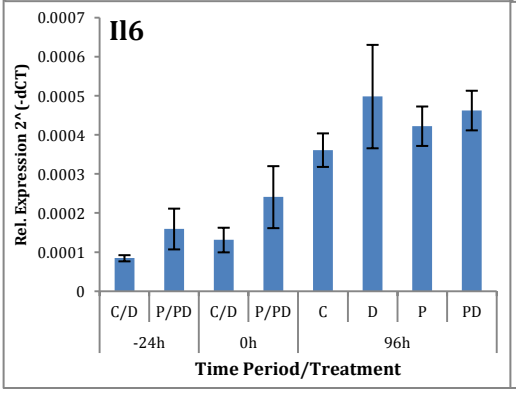

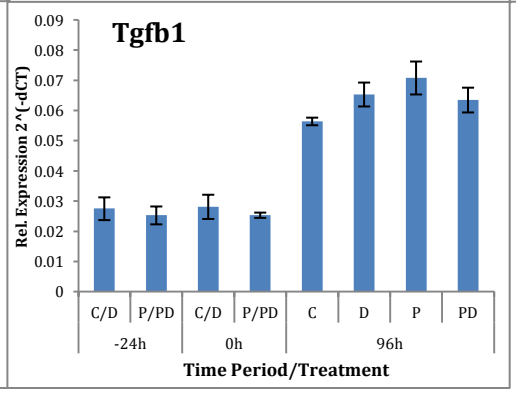

Adipoq, Lep, and Mstn not shown because they were below the detectable limit for all time points.

Proteomic analysis of the testosterone depleted proliferation and differentiation programs- A four-way Venn diagram was constructed based on the major proteins present at the 0h and 96h time points for each treatment group. A pairwise comparison was made between the 96h period of the treatment group and its 0h time point. The pairwise comparisons were then gathered, and a four-way Venn diagram constructed that showed the common proteins between the pairwise comparisons. The numbers of common proteins present were as follows:

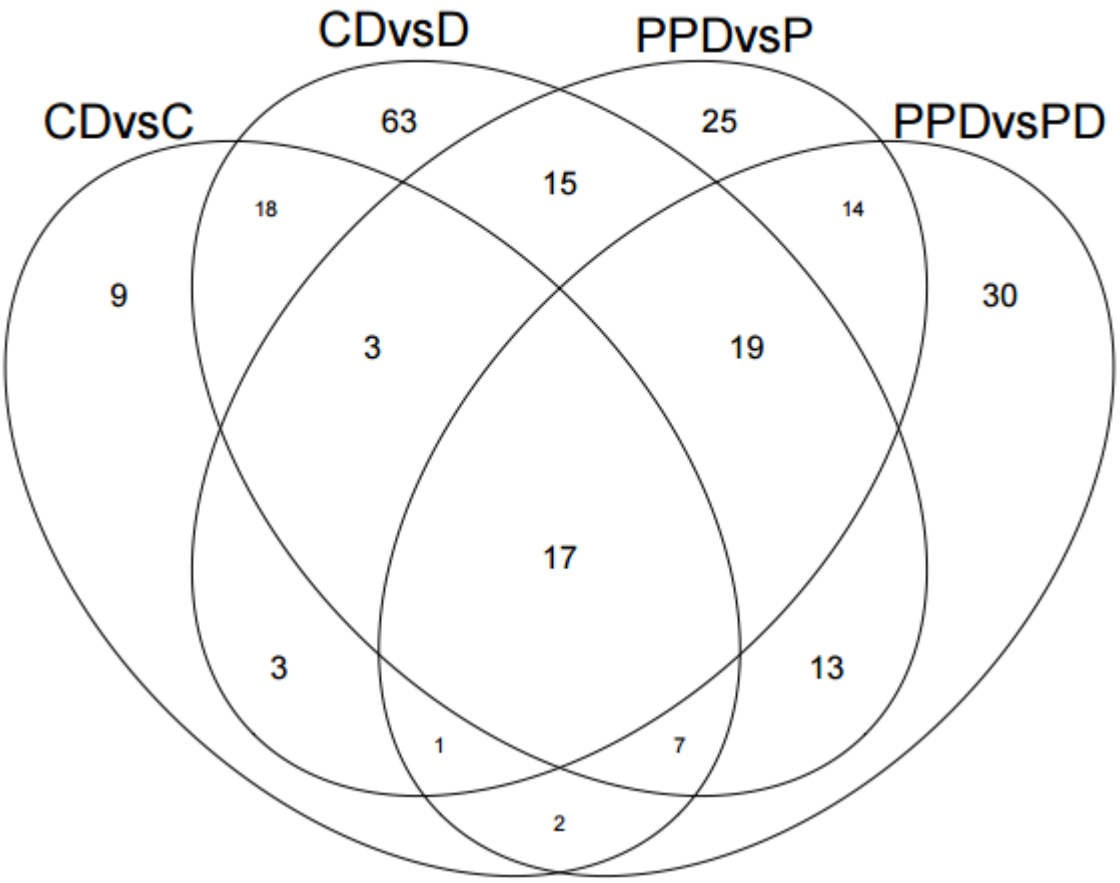

Figure 11: 4-way Venn Diagram for the unique, differential expression of proteins with the 3 treatment groups, and the control group. The comparisons are 96h to 0h for each respective group. CDvsC is the control group, CDvsD is testosterone depletion during differentiation,

PPDvsP is testosterone depletion during proliferation, and PPDvsPD is testosterone depletion during the entire time course.

Figure 11 displays the number of uniquely, differentially expressed proteins for the 3 treatment groups. The proteins that were differentially expressed from the 0h to 96 hour of each grouping, and exclusive to said groupings (corresponding to 9 for C/D vs. C, 63 for C/D vs. D, 25 for P/PD vs. P, and 30 for P/PD vs. PD) were:

Differentially Expressed Proteins Exclusive to the C/D vs. C Grouping		
Protein ID	**Protein**	**Gene**
UBC_MOUSE	Polyubiquitin-C	Ubc
SYNC_MOUSE	Asparagine--tRNA ligase; cytoplasmic	Nars
RL14_MOUSE	60S ribosomal protein L14	Rpl14
EIF3A_MOUSE	Eukaryotic translation initiation factor 3 subunit A	Eif3a
E41L2_MOUSE	Band 4.1-like protein	Epb41l2
PSME2_MOUSE	Proteasome activator complex subunit 2	Psme2
RCC1_MOUSE	Regulator of chromosome condensation	Rcc1
GSTM7_MOUSE	Glutathione S-transferase Mu 7	Gstm7
GSTM2_MOUSE	Glutathione S-transferase Mu 2	Gstm2

Differentially Expressed Proteins Exclusive to the C/D vs. D Grouping		
Protein ID	**Protein**	**Gene**
TBB3_MOUSE	Tubulin beta-3 chain	Tubb3
ANXA2_MOUSE	Annexin A2	Anxa2
ANXA1_MOUSE	Annexin A1	Anxa1
MYH1_MOUSE	Myosin-1	Myh1
ENOB_MOUSE	Beta-enolase	Eno3
MYH7_MOUSE	Myosin-7	Myh7
1433B_MOUSE	14-3-3 protein beta/alpha	Ywhab
TCPB_MOUSE	T-complex protein 1 subunit beta	Cct2
TCPE_MOUSE	T-complex protein 1 subunit epsilon	Cct5
MACF1_MOUSE	Microtubule-actin cross-linking factor 1	Macf1
MYO1C_MOUSE	Unconventional myosin-Ic	Myo1c
TCPZ_MOUSE	T-complex protein 1 subunit zeta	Cct6a
BASP1_MOUSE	Brain acid soluble protein 1	Basp1
PUR9_MOUSE	Bifunctional purine biosynthesis protein PURH	Atic
RS3A_MOUSE	40S ribosomal protein S3a	Rps3a
HSP74_MOUSE	Heat shock 70 kDa protein 4	Hspa4
PRDX6_MOUSE	Peroxiredoxin-6	Prdx6
RS10_MOUSE	40S ribosomal protein S10	Rps10
TRI72_MOUSE	Tripartite motif-containing protein 72	Trim72
RS3_MOUSE	40S ribosomal protein S3	Rps3
RL3_MOUSE	60S ribosomal protein L3	Rpl3

CALX_MOUSE	Calnexin	Canx
AATM_MOUSE	Aspartate aminotransferase; mitochondrial	Got2
RINI_MOUSE	Ribonuclease inhibitor	Rnh1
U5S1_MOUSE	116 kDa U5 small nuclear ribonucleoprotein component	Eftud2
PTRF_MOUSE	Polymerase I and transcript release factor	Ptrf
PRDX2_MOUSE	Peroxiredoxin-2	Prdx2
SYK_MOUSE	Lysine--tRNA ligase	Kars
MPCP_MOUSE	Phosphate carrier protein; mitochondrial	Slc25a3
TKT_MOUSE	Transketolase	Tkt
EIF3B_MOUSE	Eukaryotic translation initiation factor 3 subunit B	Eif3b
IPO7_MOUSE	Importin-7	Ipo7
LRRF1_MOUSE	Leucine-rich repeat flightless-interacting protein 1	Lrrfip1
EIF3C_MOUSE	Eukaryotic translation initiation factor 3 subunit C	Eif3c
SUGT1_MOUSE	Suppressor of G2 allele of SKP1 homolog	Sugt1
ESYT1_MOUSE	Extended synaptotagmin-1	Esyt1
IF4B_MOUSE	Eukaryotic translation initiation factor 4B	Eif4b
HNRPC_MOUSE	Heterogeneous nuclear ribonucleoproteins C1/C2	Hnrnpc
TAGL3_MOUSE	Transgelin-3	Tagln3
MARE1_MOUSE	Microtubule-associated protein RP/EB family member 1	Mapre1
EHD1_MOUSE	EH domain-containing protein 1	Ehd1
ODPA_MOUSE	Pyruvate dehydrogenase E1 component subunit alpha; somatic form; mitochondrial	Pdha1
RAB10_MOUSE	Ras-related protein Rab-10	Rab10
ACADL_MOUSE	Long-chain specific acyl-CoA dehydrogenase; mitochondrial	Acadl
UAP1L_MOUSE	UDP-N-acetylhexosamine pyrophosphorylase-like protein 1	Uap1l1
RL21_MOUSE	60S ribosomal protein L21	Rpl21
CATZ_MOUSE	Cathepsin Z	Ctsz
ASNS_MOUSE	Asparagine synthetase [glutamine-hydrolyzing]	Asns
TSP1_MOUSE	Thrombospondin-1	Thbs1
CN166_MOUSE	UPF0568 protein C14orf166 homolog	N/A
MVP_MOUSE	Major vault protein	Mvp
PSME3_MOUSE	Proteasome activator complex subunit 3	Psme3
EPHA2_MOUSE	Ephrin type-A receptor 2	Epha2
LIMA1_MOUSE	LIM domain and actin-binding protein 1	Lima1
HS105_MOUSE	Heat shock protein 105 kDa	Hsph1
SNX1_MOUSE	Sorting nexin-1	Snx1
PTGR1_MOUSE	Prostaglandin reductase 1	Ptgr1
SPR1A_MOUSE	Cornifin-A	Sprr1a
ABCF2_MOUSE	ATP-binding cassette sub-family F member 2	Abcf2
XRCC6_MOUSE	X-ray repair cross-complementing protein 6	Xrcc6
RB11B_MOUSE	Ras-related protein Rab-11B	Rab11b
PP1R7_MOUSE	Protein phosphatase 1 regulatory subunit 7	Ppp1r7
MY18A_MOUSE	Unconventional myosin-XVIIIa	Myo18a

Differentially Expressed Proteins Exclusive to the P/PD vs. P Grouping		
Protein ID	**Protein**	**Gene**
ACTN3_MOUSE	Alpha-actinin-3	Actn3
RTN4_MOUSE	Reticulon-4	Rtn4
DDX3Y_MOUSE	ATP-dependent RNA helicase DDX3Y	Ddx3y
MYBPH_MOUSE	Myosin-binding protein H	Mybph
SRCA_MOUSE	Sarcalumenin	Srl
SAHH_MOUSE	Adenosylhomocysteinase	Ahcy
PACN2_MOUSE	Protein kinase C and casein kinase substrate in neurons protein 2	Pacsin2
ETFB_MOUSE	Electron transfer flavoprotein subunit beta	Etfb
FAS_MOUSE	Fatty acid synthase	Fasn
TXND5_MOUSE	Thioredoxin domain-containing protein 5	Txndc5
ATP5H_MOUSE	ATP synthase subunit d; mitochondrial	Atp5h
USO1_MOUSE	General vesicular transport factor p115	Uso1
RS11_MOUSE	40S ribosomal protein S11	Rps11
SYP2L_MOUSE	Synaptopodin 2-like protein	Synpo2l
TNNI1_MOUSE	Troponin I; slow skeletal muscle	Tnni1
GPDM_MOUSE	Glycerol-3-phosphate dehydrogenase; mitochondrial	Gpd2
GATM_MOUSE	Glycine amidinotransferase; mitochondrial	Gatm
CO1A2_MOUSE	Collagen alpha-2(I) chain	Col1a2
TNNT2_MOUSE	Troponin T; cardiac muscle	Tnnt2
TMM43_MOUSE	Transmembrane protein 43	Tmem43
MCM6_MOUSE	DNA replication licensing factor MCM6	Mcm6
CDK4_MOUSE	Cyclin-dependent kinase 4	Cdk4
THIM_MOUSE	3-ketoacyl-CoA thiolase; mitochondrial	Acaa2
TNNT3_MOUSE	Troponin T; fast skeletal muscle	Tnnt3
CDK13_MOUSE	Cyclin-dependent kinase 13	Cdk13

Differentially Expressed Proteins Exclusive to the PD/P vs. PD Grouping		
Protein ID	**Protein**	**Gene**
HS90B_MOUSE	Heat shock protein HSP 90-beta	Hsp90ab1
TAGL_MOUSE	Transgelin	Tagln
NPM_MOUSE	Nucleophosmin	Npm1
LRC59_MOUSE	Leucine-rich repeat-containing protein 59	Lrrc59
STIP1_MOUSE	Stress-induced-phosphoprotein 1	Stip1
LMNB1_MOUSE	Lamin-B1	Lmnb1
ANXA4_MOUSE	Annexin A4	Anxa4
RS13_MOUSE	40S ribosomal protein S13	Rps13
RL7A_MOUSE	60S ribosomal protein L7a	Rpl7a
SPTB2_MOUSE	Spectrin beta chain; non-erythrocytic 1	Sptbn1
TYB4_MOUSE	Thymosin beta-4	Tmsb4x
IF4G1_MOUSE	Eukaryotic translation initiation factor 4 gamma 1	Eif4g1
THIO_MOUSE	Thioredoxin	Txn
C1TC_MOUSE	C-1-tetrahydrofolate synthase; cytoplasmic	Mthfd1
RAGP1_MOUSE	Ran GTPase-activating protein 1	Rangap1
CALU_MOUSE	Calumenin	Calu
PPIC_MOUSE	Peptidyl-prolyl cis-trans isomerase C	Ppic
NOP2_MOUSE	Putative ribosomal RNA methyltransferase NOP2	Nop2
VAT1_MOUSE	Synaptic vesicle membrane protein VAT-1 homolog	Vat1
GNAI2_MOUSE	Guanine nucleotide-binding protein G(i) subunit alpha-2	Gnai2
NDRG1_MOUSE	Protein NDRG1	Ndrg1
ODPB_MOUSE	Pyruvate dehydrogenase E1 component subunit beta; mitochondrial	Pdhb
SC23A_MOUSE	Protein transport protein Sec23A	Sec23a
KAD2_MOUSE	Adenylate kinase 2; mitochondrial	Ak2
RL9_MOUSE	60S ribosomal protein L9	Rpl9
NCAM1_MOUSE	Neural cell adhesion molecule 1	Ncam1
CTNB1_MOUSE	Catenin beta-1	Ctnnb1
SAFB1_MOUSE	Scaffold attachment factor B1	Safb
VMA5A_MOUSE	von Willebrand factor A domain-containing protein 5A	Vwa5a
SC22B_MOUSE	Vesicle-trafficking protein SEC22b	Sec22b

E. Discussion

Upstream Regulators of differentiation - The determination of key pathway changes during the differentiation program was of utmost importance, so that the testosterone depletion study had a baseline to compare. Serum response factor (SRF), insulin signaling, and p53 were identified as regulators of the differentiation process in our IPA analysis. SRF has been shown to modulate differentiation through activation-motivated binding of myogenin and MyoD[18]. SRF also has the ability to bind to the AR and facilitate myogenesis through activation of myogenic genes within the nucleus[19].

p53 is a crucial trigger to muscle cell differentiation[20], and acts through the retinoblastoma protein (pRb). In order for myoblasts to differentiate, they must exit the cell cycle. p53 activates pRb which causes cell cycle withdrawal, and induction into the differentiation program[21]. Continued expression of pRb keeps the differentiating myoblasts from re-entering the cell cycle, thus p53 is critical to the activation of the differentiation program.

The insulin-like growth factor 1 receptor (IGF-IR) has been shown to play a role in the proliferation and differentiation of myoblasts[22] through binding of insulin-like growth factor-II (IGF-II). IGF-1 also plays a crucial role during the cell cycle through positive regulation of the mTOR signaling pathway[23, 24]. To further the discussion, insulin-like growth factor binding proteins (IGFBP) have the ability to bind to IGF molecules, and inhibit the binding of IGF to the receptor[25]. IGFBP5 specifically binds to IGF-II to restrict signaling to the IGF receptors, which stalls proliferation and differentiation of myoblasts[25]. On the contrary, IGFBP5 binds IGF-I to stimulate myogenesis[25]. The roles of IGFBP5, IGF-I, and IGF-II are important to the understanding of the proliferation and differentiation processes within skeletal muscles, and seem to provide pathways by which the differentiation program can be activated.

Through the identification of the key regulators during the differentiation program, we are better able to study the exact mechanisms of T depletion on myogenesis.

Implications of testosterone depletion during differentiation –

Pax7 and Myogenin:

An important part of the differentiation process is the change from a Pax7 expressing myoblast[6] into a myogenin expressing myocyte and eventually a myotube. Muscle cells must undergo this Pax7 maturation process in order to become fully differentiated myotubes[11]. Pax7 expression is not detectable in fully differentiated myotubes[11, 26], and is down-regulated in order for differentiation to occur. The Pax7 proliferation process is critical to the development of myotubes, and the down-regulation coupled with the de-expression of Pax7 protein allows for terminal differentiation to occur[26]. Within our cultures, both the D and PD treatment groups – which both were depleted of T during the differentiation process – presented with up-regulated Pax7 expression at the 96h time point coupled with down-regulated myogenin. The trend of Pax7 up-regulation and myogenin down-regulation at the peak of differentiation suggests that when the culture was depleted of T during the differentiation period, the cells were unable to fuse in order to form multinucleated myotubes, and were essentially in a state of continued proliferation.

Insulin-Like Growth Factor Signaling:

IGF signaling plays a role in both the proliferation and differentiation of myoblasts as previously stated. The increased expression of IGF-1 in 96h time point of testosterone depletion alongside the Pax7 up-regulation and myogenin down-regulation further suggests that a proliferative state

is ongoing. IGF-1 acts as a mitogen in the mTOR signaling pathway[23], and thus the increased expression could point towards a continued activation of this pathway, and a continued proliferative state. Further research into the interactions of IGF-I and testosterone must be used to clarify the impact of IGF-I on endocrine signaling, along with its specific role in the muscle differentiation and proliferation processes.

Acta1 (alpha actin 1), Myh1 (myosin heavy chain 1), and Myh2 (myosin heavy chain 2):

A combination of actin and myosin filaments in skeletal muscle allow for muscle contractions[27]. The combined action of myosin sliding past actin filaments contracts the muscles, and generates force. Acta1 mutations in humans are associated with myopathy and muscle weakness[28]. Mutations to the Acta1 gene are characteristic to nemaline myopathy, which leads to weakness of the arms, legs, and trunk muscles. Alpha-actin 1 was shown to be down-regulated at the 96h time point when T was depleted during differentiation, which suggests the muscles possess a reduced ability to contract. Acta1 when under-expressed could lead to myopathy type states, but further research must be employed to verify.

Heat Shock Protein and AR Signaling:

Heat shock protein 90 (HSP90) is bound to AR without ligand while in the cytoplasm, and increases the AR's affinity to binding of hormones[29]. While bound to HSP90 the AR cannot bind to DNA [29], and must dissociate first through androgen binding. Once androgens bind, HSP90 assists in transforming the AR into a DNA-binding state[30, 31], and HSP90 also helps transfer the AR to the nucleus so that the AR can activate target genes[32]. The highest count protein that was differentially expressed proteomically at the 96h of the PD group was HSP90.

The high-count state of HSP90 could point towards a stalled growth process of the myoblasts, because there are no androgens available to bind to the AR, and cause translocation to the nucleus for differentiation activation. Further investigation into this mechanism is necessary to confirm our ideas.

F. Conclusions

The study presented here provided a vast array of data that provides a thorough basis for further studies to be designed. The regulators of differentiation have been identified and qualitatively correlated with their proposed function in regards to testosterone depletion, and a possible biomarker for testosterone status has been identified in HSP90. The basis set of data, which is comprised of proteomic, transcriptional, and pathway analyses, provides a multitude of future directions, and the molecular mechanisms of testosterone depletion are being unraveled, and will continue to be determined in the near future.

G. Future Directions

Due to the exploratory nature of our investigation, the amount of data collected provides for multiple further analyses. The first direction is identifying the AR within the nucleus versus the AR in the cytoplasm of the differentiation phase testosterone-depleted cells at 96h. HSP90 wil be measured to find the correlation between the AR bound HSP90 and unbound nucleus-localized AR.

The next possible investigation is into the specific link between T and insulin signaling pathways, determining the common link that connects these two pathways. We propose that the AR is the common link, but this must be studied further.

Metabolomics of the cells under the depletion conditions is of utmost interest. IPA identified key metabolic pathways changing during the differentiation program, namely glycolysis, beta-oxidation, and the TCA cycle. Metabolomics could provide a biomarker for testosterone status that could be translated to drug testing, as well as muscle function in patients.

Lastly, pharmacological ADT agents will be tested in culture to determine if they have their own specific mechanisms of action on myoblasts, separate from testosterone depletion solely. Essentially ADT drugs inhibit the production or signaling of androgens, such as testosterone, through the androgen receptor (AR), which in turn inhibits the proliferation of testosterone sensitive tissues, including prostate cancer and muscle. A diagram of the androgen signaling process is pictured above (pg. 2), including the specific mechanisms of action of clinically relevant ADT agents. However the specific impact of the AR targeting agents on skeletal muscle has not been well studied.

References

1. Alibhai, S.M., et al., *Long-term impact of androgen-deprivation therapy on physical function and quality of life.* Cancer, 2015.
2. Denmeade, S.R. and J.T. Isaacs, *A history of prostate cancer treatment.* Nat Rev Cancer, 2002. **2**(5): p. 389-96.
3. Bhasin, S., L. Woodhouse, and T.W. Storer, *Proof of the effect of testosterone on skeletal muscle.* J Endocrinol, 2001. **170**(1): p. 27-38.
4. *What are the key statistics about prostate cancer?* 2015 3/12/2015; Available from: http://www.cancer.org/cancer/prostatecancer/detailedguide/prostate-cancer-key-statistics.
5. Leitzmann, M.F. and S. Rohrmann, *Risk factors for the onset of prostatic cancer: age, location, and behavioral correlates.* Clin Epidemiol, 2012. **4**: p. 1-11.
6. Olguin, H.C. and B.B. Olwin, *Pax-7 up-regulation inhibits myogenesis and cell cycle progression in satellite cells: a potential mechanism for self-renewal.* Dev Biol, 2004. **275**(2): p. 375-88.

7. Perdiguero, E., et al., *Epigenetic regulation of myogenesis.* Epigenetics, 2009. **4**(8): p. 541-50.
8. Bhasin, S., et al., *Testosterone replacement increases fat-free mass and muscle size in hypogonadal men.* J Clin Endocrinol Metab, 1997. **82**(2): p. 407-13.
9. Lee, D.K., *Androgen receptor enhances myogenin expression and accelerates differentiation.* Biochem Biophys Res Commun, 2002. **294**(2): p. 408-13.
10. Dubois, V., et al., *Androgens and skeletal muscle: cellular and molecular action mechanisms underlying the anabolic actions.* Cell Mol Life Sci, 2012. **69**(10): p. 1651-67.
11. Diel, P., et al., *C2C12 myoblastoma cell differentiation and proliferation is stimulated by androgens and associated with a modulation of myostatin and Pax7 expression.* J Mol Endocrinol, 2008. **40**(5): p. 231-41.
12. Saad, F., *Evidence for the efficacy of enzalutamide in postchemotherapy metastatic castrate-resistant prostate cancer.* Ther Adv Urol, 2013. **5**(4): p. 201-10.
13. Storer, T.W., R. Miciek, and T.G. Travison, *Muscle function, physical performance and body composition changes in men with prostate cancer undergoing androgen deprivation therapy.* Asian J Androl, 2012. **14**(2): p. 204-21.
14. Wannenes, F., et al., *Androgen receptor expression during C2C12 skeletal muscle cell line differentiation.* Mol Cell Endocrinol, 2008. **292**(1-2): p. 11-9.
15. Kislinger, T., et al., *Proteome dynamics during C2C12 myoblast differentiation.* Mol Cell Proteomics, 2005. **4**(7): p. 887-901.
16. Pirmoradian, M., et al., *Rapid and deep human proteome analysis by single-dimension shotgun proteomics.* Mol Cell Proteomics, 2013. **12**(11): p. 3330-8.
17. Tan, H.L., et al., *beta-Carotene-9',10'-oxygenase status modulates the impact of dietary tomato and lycopene on hepatic nuclear receptor-, stress-, and metabolism-related gene expression in mice.* J Nutr, 2014. **144**(4): p. 431-9.
18. Groisman, R., et al., *Physical interaction between the mitogen-responsive serum response factor and myogenic basic-helix-loop-helix proteins.* J Biol Chem, 1996. **271**(9): p. 5258-64.
19. Vlahopoulos, S., et al., *Recruitment of the androgen receptor via serum response factor facilitates expression of a myogenic gene.* J Biol Chem, 2005. **280**(9): p. 7786-92.
20. Cam, H., et al., *p53 family members in myogenic differentiation and rhabdomyosarcoma development.* Cancer Cell, 2006. **10**(4): p. 281-93.
21. Porrello, A., et al., *p53 regulates myogenesis by triggering the differentiation activity of pRb.* J Cell Biol, 2000. **151**(6): p. 1295-304.
22. Bach, L.A., R. Salemi, and K.S. Leeding, *Roles of insulin-like growth factor (IGF) receptors and IGF-binding proteins in IGF-II-induced proliferation and differentiation of L6A1 rat myoblasts.* Endocrinology, 1995. **136**(11): p. 5061-9.
23. Nader, G.A., T.J. McLoughlin, and K.A. Esser, *mTOR function in skeletal muscle hypertrophy: increased ribosomal RNA via cell cycle regulators.* Am J Physiol Cell Physiol, 2005. **289**(6): p. C1457-65.
24. Miyazaki, M. and K.A. Esser, *Cellular mechanisms regulating protein synthesis and skeletal muscle hypertrophy in animals.* J Appl Physiol (1985), 2009. **106**(4): p. 1367-73.

25. Ewton, D.Z., et al., *Modulation of insulin-like growth factor actions in L6A1 myoblasts by insulin-like growth factor binding protein (IGFBP)-4 and IGFBP-5: a dual role for IGFBP-5.* J Cell Physiol, 1998. **177**(1): p. 47-57.
26. Zammit, P.S., et al., *Pax7 and myogenic progression in skeletal muscle satellite cells.* J Cell Sci, 2006. **119**(Pt 9): p. 1824-32.
27. Cooper, G., *Actin, Myosin, and Cell Movement*, in *The Cell: A molecular Approach*. 2000, Sinauer Associates: Sunderland, MA.
28. Nowak, K.J., et al., *Mutations in the skeletal muscle alpha-actin gene in patients with actin myopathy and nemaline myopathy.* Nat Genet, 1999. **23**(2): p. 208-12.
29. Fang, Y., et al., *Hsp90 regulates androgen receptor hormone binding affinity in vivo.* J Biol Chem, 1996. **271**(45): p. 28697-702.
30. Prescott, J. and G.A. Coetzee, *Molecular chaperones throughout the life cycle of the androgen receptor.* Cancer Lett, 2006. **231**(1): p. 12-9.
31. Veldscholte, J., et al., *Hormone-induced dissociation of the androgen receptor-heat-shock protein complex: use of a new monoclonal antibody to distinguish transformed from nontransformed receptors.* Biochemistry, 1992. **31**(32): p. 7422-30.
32. Georget, V., et al., *Mechanism of antiandrogen action: key role of hsp90 in conformational change and transcriptional activity of the androgen receptor.* Biochemistry, 2002. **41**(39): p. 11824-31.